

e.2



Lawrence Berkeley Laboratory

UNIVERSITY OF CALIFORNIA

Materials & Chemical Sciences Division

RECEIVED
LIBRARY
SEPTEMBER 23 1987

NOV 20 1987

LIBRARY AND
DOCUMENTS SECTION

Fundamental Studies of Catalytic Gasification: Annual Report, October 1, 1986–September 30, 1987

H. Heinemann

September 1987

TWO-WEEK LOAN COPY

*This is a Library Circulating Copy
which may be borrowed for two weeks.*



LBL-23930
e.2

DISCLAIMER

This document was prepared as an account of work sponsored by the United States Government. While this document is believed to contain correct information, neither the United States Government nor any agency thereof, nor the Regents of the University of California, nor any of their employees, makes any warranty, express or implied, or assumes any legal responsibility for the accuracy, completeness, or usefulness of any information, apparatus, product, or process disclosed, or represents that its use would not infringe privately owned rights. Reference herein to any specific commercial product, process, or service by its trade name, trademark, manufacturer, or otherwise, does not necessarily constitute or imply its endorsement, recommendation, or favoring by the United States Government or any agency thereof, or the Regents of the University of California. The views and opinions of authors expressed herein do not necessarily state or reflect those of the United States Government or any agency thereof or the Regents of the University of California.

ANNUAL REPORT

October 1, 1986 - September 30, 1987

FUNDAMENTAL STUDIES OF CATALYTIC GASIFICATION

Principal Investigator: Heinz Heinemann

Lawrence Berkeley Laboratory
University of California
Berkeley, CA 94720

This work was supported by the Assistant Secretary for Fossil Energy, Office of Technical Coordination, U.S. Department of Energy under Contract DE-AC03-76SF00098, through the Morgantown Energy Technology Center, Morgantown, West Virginia 26505.

TABLE OF CONTENTS

	<u>Page</u>
I Task Description for Fiscal year 1987	1
II Highlights.	1
III Progress of Studies	6
a) Kinetic Studies.	6
b) Studies of Surface Species	9
c) Adsorption and TPD Studies	12
IV Appendix A.	18
V Appendix B.	46

I. Task Description for FY 1987

This program studies the basic chemistry of the reaction of carbonaceous materials with water in the presence of catalysts to produce hydrogen and/or synthesis gas. Relatively low temperatures are being used. The catalysts under investigation are compounds of potassium and a transition metal oxide. Major objectives are the extension of the work from chars to coke; the effect of H_2 , CO and CO_2 partial pressure on the gaseous product distribution; and the inhibition of catalyst poisoning by ash components.

II. Highlights

1. Activation energies for K/Ni catalysed steam gasification of graphite and of chars are identical, indicating the same mechanism prevails though rates are much higher for chars. This permits extrapolation of findings in high vacuum equipment from graphite to chars.
2. The kinetic properties of a catalyst derived from a mixture of KOH and $Ni(NO_3)_2$ for steam gasification of three chars have been determined. H_2 , CO_2 and small amounts of CO and CH_4 are the reaction products. The product distribution is controlled by the activation energies for formation of the gases. The activation energies for H_2 and CO_2 formation are 29 and 36 Kcal/mol respectively. The catalyst derived from the $KOH/Ni(NO_3)_2$

mixture has better catalytic properties, due to a cooperative effect between nickel and potassium, than catalyst derived by loading the components alone. The mixture has a higher activity and lower activation energies for H_2 and CO_2 production than KOH alone, and higher resistance to deactivation than $Ni(NO_3)_2$ alone.

3. The gasification of graphite by H_2O vapor, wet H_2 and wet O_2 , catalyzed by a Ni/K mixture has been studied using controlled atmosphere electron microscopy (CAEM). In H_2O vapor the carbon consumption, between 550 and 1100 C, is catalyzed by an edge recession mode of attack in the [1120] direction, with no sign of deactivation. An activation energy of 30.8 ± 0.9 Kcal/mol was obtained in this case. In wet H_2 both channeling and edge recession occur simultaneously. The activation energy obtained was equal to 30 ± 2 Kcal/mol. The catalyst deactivates above 1000 C, but can be regenerated by treating the sample in H_2O vapor at 60 C. In wet O_2 , graphite is also gasified by edge recession, but no preferred direction was observed. The catalyst maintains its activity up to 1000 C, and an activation energy of 25 ± 2 Kcal/mol was obtained. These results show that the catalytic properties of the Ni/K mixture are superior to those of Ni and K alone due to a cooperative effect between the components.
4. Comparison of K/Ni catalyst for steam gasification of Illinois #6 char with K or Ni alone indicates K alone produces much higher

CO/CO₂ ratios than K/Ni (3.5 vs. 0.8) and therefore less hydrogen; activation energies for K catalyst are much higher than for K/Ni. Ni alone is almost inactive for the steam gasification of Illinois #6 except for the short first period of operation. The H₂ production rate for Ni alone as in the case of K alone is lower than that for K/Ni.

5. The CO/CO₂ ratio of gases produced in the presence of a K/Ni catalyst along with hydrogen varies with different chars. The ratio is 0.8 for Illinois #6 char and 0.08 for North Dakota char. Methane production is several orders of magnitude smaller and ceases after about 2 hours.
6. North Dakota char, which showed higher gasification rates than other chars tested exhibited some activity even in the absence of an added K/Ni catalyst. However, this innate activity died within a few hours.
7. North Dakota char was treated with steam until it was inactive and then a K/Ni catalyst was added. Gasification now occurred at a higher rate than the initial one with the untreated char and deactivation was extremely slow. About 40% of the char was gasified in 2 hours. A totally demineralized char had no activity. Ni on this char had only slight activity, but Ni/K allowed 100% char consumption in 2 hours.
8. Deactivation of Ni/K containing char does not appear to be a function of reduced porosity or surface of the char during

gasification, but of catalyst poisoning by ash components which can be deactivated by steaming.

9. An investigation of the effect of catalyst loading between the previously used 1 mole% on carbon and 3% indicates that the rate of H₂ production increases five fold when the Ni/C ratio (at constant Ni/K of 1) increases from 1 to 2.5×10^{-2} and increases six fold when the Ni/C ratio increases from 1 to 3.2×10^{-2} .
10. Work is underway with demineralized chars to determine the effect of ash on the catalyst deactivation rate.
11. It has been found that the NiO/KOH catalyst is very active for the Boudouard reaction. Experiments were carried out with CO₂ in the absence of water.
12. The NiO/KOH catalyst promotes the hydrogenation of CO to methane in the absence of water at 673K and above. Since CO₂ can be reduced to CO by char, CO₂ can also go to methane.
13. An XPS study of surface species on graphite after impregnation with KOH and/or NiNO₃ before and after gasification confirmed the chemical interaction of potassium and nickel compounds.
 - a) nickel stabilizes potassium on the surface.

- b) nickel alone, a brief lived very active catalyst, becomes deactivated because it cannot wet the carbon surface. In the presence of potassium, wetting takes place.
- c) most of the nickel in the K/Ni catalyst is present in the Ni(+2) form, which is not reduced by carbon or hydrogen. It is possible that there is a very small amount (>2%) of metallic nickel present in the NiO. It is also possible that under the influence of KOH or NiO(OH) a Ni(+3) is formed, which may dissociate water.

14. Prior to an attempt to determine the surface species on carbonaceous materials formed by reaction with either CO, CO₂, O₂ or H₂O, experiments on adsorption and temperature programmed desorption (TPD) were carried out with graphite. CO, CO₂, O₂ and H₂O chemisorption yield the same CO desorption precursor on three different sites, decomposing at 700, 820 and 980°C. This species has been tentatively assigned to a semi-quinone functional group. As by-products of the CO precursor, CO₂ adsorption gives gaseous CO, and H₂O adsorption gives hydrogen atoms that either recombine to form H₂, or form carbon-hydrogen bonds of two types, aromatic like and aliphatic like. The first type decomposes around 1000C to produce H₂, and the second produces hydrocarbons below 500°C.

A small fraction of the CO precursors reacts with the adsorbing gas to produce the CO₂ precursor, which then decomposes

thermally between 200 and 600°C. A lactone species has been proposed as the CO₂ surface precursor.

CO adsorbed at room temperature leads to the formation of a weakly bound species, assigned to a carbonyl group, and desorbs at 200°C as CO. Physical wetting by water also leads to a weakly bound species, suggested to be a hydrate, and desorbs at 350°C as H₂O.

III. Progress of Studies

Many of the results summarized in the "Highlights" section of this report have been discussed in detail in the Quarterly Reports of January 1 and April 1, 1987. This section deals with work performed during the second half of fiscal 1987.

a) Kinetic Studies

Work described on char steam gasification in earlier reports showed that potassium-nickel catalysts were active at relatively low temperatures (800-900 K) in promoting the rate of hydrogen production. However, the catalytic activity declined as a function of time. It was also shown that treatment of the char with aqua regia prior to impregnation with K/Ni resulted in a somewhat lower but steady activity. Questions were raised whether this might be due to partial oxidation of the char rather than

demineralization. The earlier data also showed that the CO_2/CO ratio of production gas and, therefore, the amount of H_2 production varied from char to char, possibly due to participation of ash components in the catalysis..

North Dakota char had been shown to be easier to gasify than three other chars. Therefore, new experiments were carried out with this char.

Using the char without impregnation with any catalyst, it was found that fairly rapid initial hydrogen production occurred at 890 K with a CO_2/CO ratio of 9. Using 1 atm. of water and 0.5 g of char a total of 30% of the char gasified in 24 hours (Fig. 1). However, the rate of hydrogen production per minute declined rapidly from 0.72 to 0.5 in less than 3 hours and to less than 0.25 in 20 hours. No gasification was obtained after 24 hours.

A new batch of the North Dakota char was then treated with steam until it showed no gasification at 890 K and was then impregnated with one mole% (based on carbon) of Ni/K (1:1 Ni/K mole ratio) to give a 1.0×10^{-2} Ni/C ratio. At the previously used gasification conditions rapid gasification occurred and 40% of the char was gasified in 2 hours (compared to 30% in 24 hours without catalyst). There was only a slight decline of hydrogen production rate over the two hour period (less than 10%) and the CO_2/CO ratio varied between 8 and 10. (Fig. 2) Methane production was

negligible. In Fig. 2 the high points at 30-40 min. and the low points at 100-120 min. are unreliable because of operational difficulties.

Fig. 3 presents basically the same data as Fig. 2 but plots the rate of carbon consumption as a function of converted carbon. There is only a small reduction of rate as the amount of carbon converted increases.

It thus seems that an inherent catalytic effect of the ash in this char is poisoned or removed by steam treatment and that simultaneously the poisoning agent for K/Ni observed with fresh catalyst impregnated with K/Ni is deactivated, resulting in a steady state gasification. The poisoning previously observed therefore cannot be attributed to changes in the surface of the char changing the gasification rate. This result will have to be verified for other chars and will also have to be confirmed by using a char which has been demineralized by HF treatment. Work along these lines is in progress. At press time for this report, early data are becoming available on HF demineralized Dakota char. The char itself is not gasified at 893 K. Impregnation with Ni shows a very short lived activity. Impregnation with Ni/K gives very rapid gasification at constant rate until all carbon is consumed after only 2 hours.

Experiments were then undertaken to determine the effect of catalyst loading on the steam deactivated Dakota char. This char which showed no gasification activity was impregnated with Ni/K (molar ratio = 1) in the amounts of 1, 2.5 and 3.2 wt% based on carbon. Gasification at 890 K demonstrated an almost five fold increase in the hydrogen production rate when the loading was 2.5%

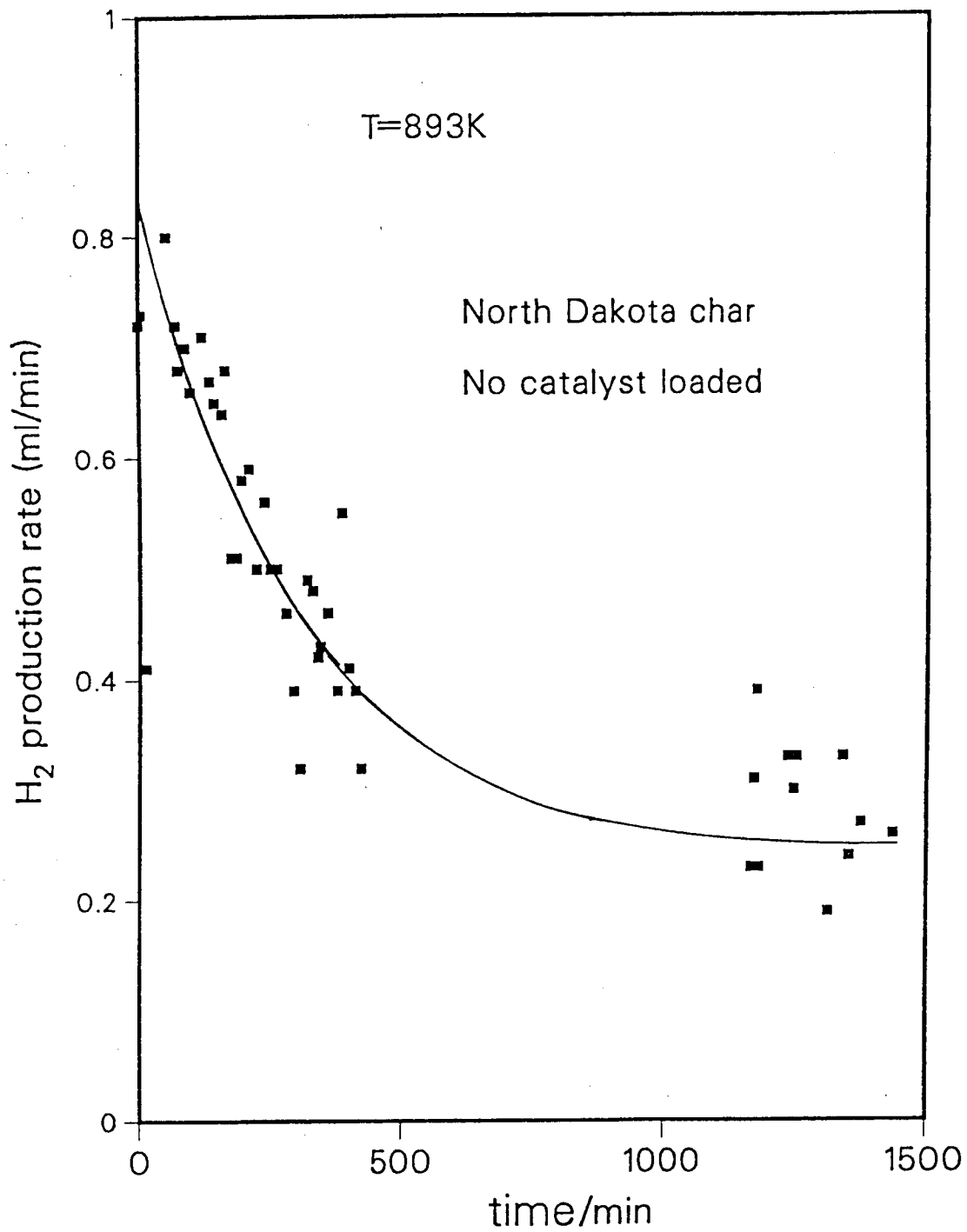


Fig. 1

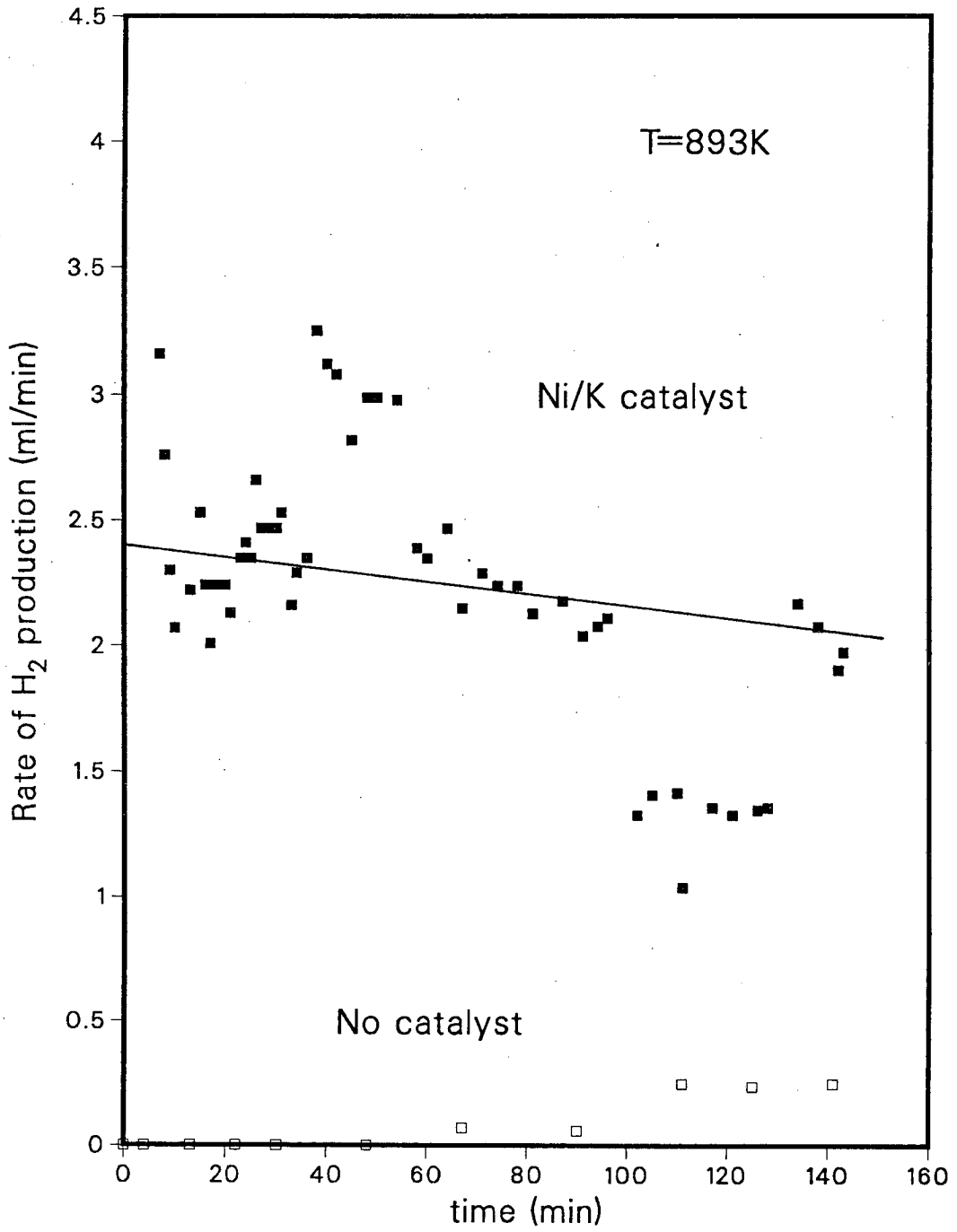


Fig. 2

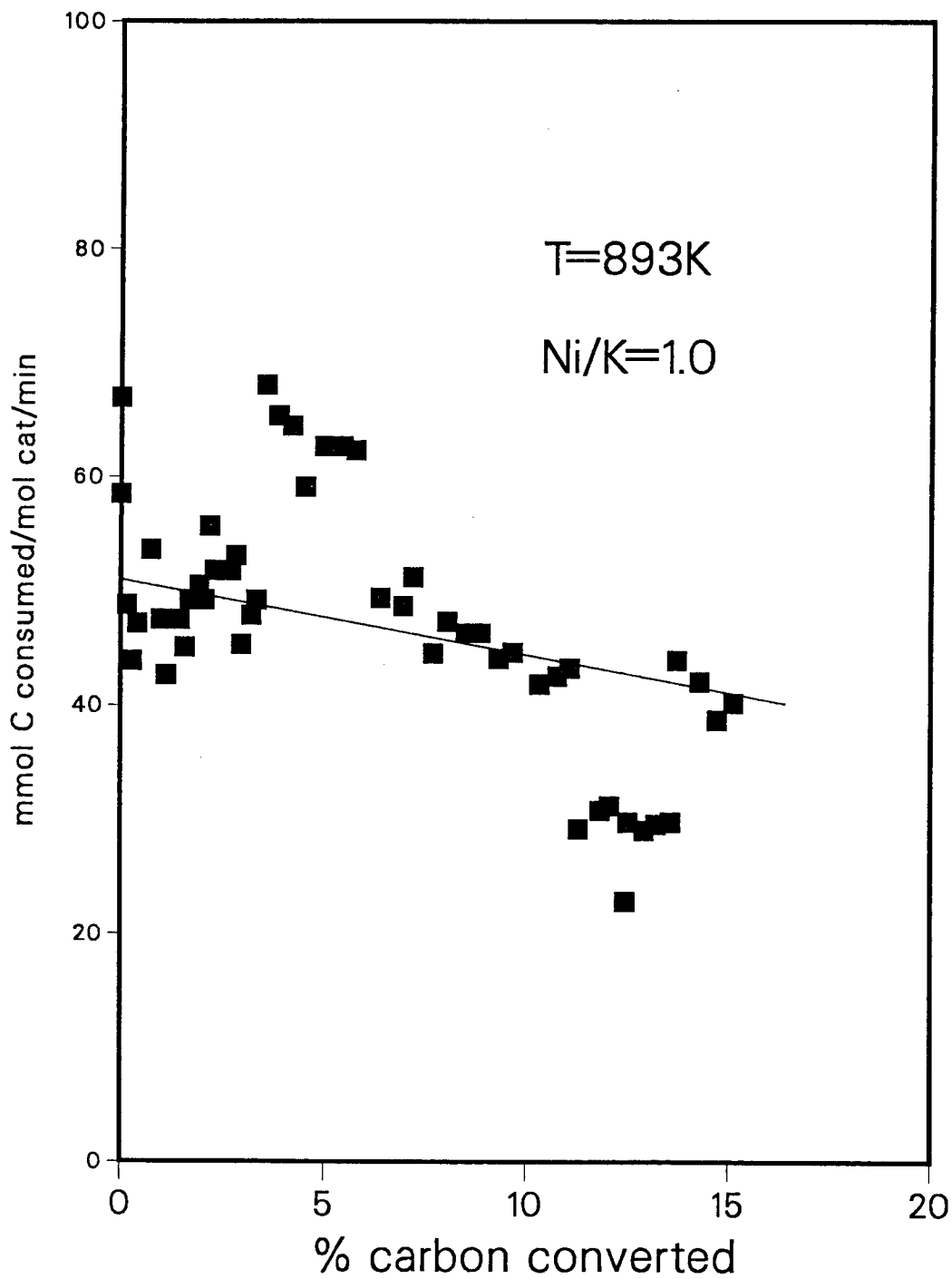


Fig. 3

TABLE 1

RATE OF H₂ PRODUCTION AS FUNCTION OF
CATALYST LOADING
Ni/K = 1.0

<u>Ni/C</u>	<u>H₂ rate ml/min</u>	<u>m mol/H₂/mol Ni/min</u>
1.0 x 10 ⁻²	0.5	49
2.5 x 10 ⁻²	2.48	97
3.2 x 10 ⁻²	2.90	89

rather than 1% and a further increase of 20% when the loading was 3.2%. The hydrogen production rate thus varied from 0.5 ml/min to 2.9 ml/min depending on the amount of catalyst on the char (Table 1). The rate of H₂ production per mol of Ni present increased substantially between Ni/C ratios of 1 and 2.5, but then decreased slightly at a ratio of 3.2.

There have also been observations that there appears to be an interaction between minerals in the ash and the ratio of Ni/K required. Data on this are presently insufficient for interpretation in this report.

b) Studies of Surface Species

Attempts have been made to better identify the nature of the interaction between potassium and nickel compounds which produces the effective catalysts used in steam gasification of chars and graphite. The study reported here involved primarily x-ray photoelectron spectroscopy (XPS) and is presented in detail in Appendix A, which is a draft of a paper for publication and is part of a Ph.D. thesis. The results of this work are particularly meaningful in connection with the Controlled Atmosphere Electronmicroscope (CAEM) study reported on pages 9-30 of the March 1987 Quarterly Report (LBL-23147). It should be pointed out that section 1.1.1 of Appendix A also appears in section III.a of this report, since the kinetic data involved are necessary for an independent understanding of Appendix A.

Since high vacuum spectroscopy cannot be undertaken with chars, all work reported in this section and in Appendix A was undertaken with graphite. The kinetic work performed in the past has shown the parallelism of catalysis in gasification of chars and of graphite with K/Ni mixtures and gives confidence that the observations of surface species on graphite are applicable to chars.

XPS data were obtained from graphite samples impregnated with KOH alone, with $\text{Ni}(\text{NO}_3)_2$ alone and with calcined mixtures of the two before and after steam gasification. Some samples were also examined after reduction in hydrogen.

- 1) Nickel nitrate on graphite forms nickel oxides on heating which can be clearly distinguished by XPS from metallic nickel. The nickel oxide is stable in steam at temperatures up to 725K. At higher temperatures (e.g. 925K) partial reduction of NiO to nickel metal occurs by means of the carbon. Steam treatment at the higher temperature leads first to complete reduction, then to reoxidation of the metal. The reoxidized nickel can only be reduced by hydrogen. During steam gasification of graphite in the presence of Ni, deactivation occurs rapidly because the carbon can no longer stabilize the Ni zero form. Additionally CAEM has shown that sintering of Ni particles occurs and carbon-nickel contact is lost.

- 2) Heat treatment of a graphite sample containing only KOH at 725K favors surface enrichment of potassium. After brief steaming at 895K the surface potassium virtually disappears. This corresponds to the loss of catalytic activity at these temperatures.

- 3) In the case of graphite samples impregnated with both KOH and $\text{Ni}(\text{NO}_3)_2$ and heat treated at 725K, potassium enrichment of the surface occurs. On steaming at 895K, some of the surface potassium is lost, but in contrast to the case of KOH impregnation alone, an appreciable amount of K remains available even after long periods. In fact after the initial steaming period no change occurs after prolonged steaming in either the oxidation state of the nickel or the surface concentration of potassium. This corresponds to the long stable activity of the catalyst after an initial activity loss and also checks with the CAEM observation of complete wetting of the crystal edges and gasification by edge recession. Nickel and potassium are uniformly distributed in the catalyst which has the high mobility of a liquid. The chemical interaction of metal and alkali may lead to a eutectic compound which lowers the melting point of NiO.

While $\text{Ni}(\text{NO}_3)_2$ impregnated graphite exhibits gasification activity only when metallic Ni is present, the

K/Ni mixture contains all or the vast majority of the nickel in the Ni(+2) state. This is true even in the presence of hydrogen.

While the activity of nickel must be due to its ability to dissociate water, the question arises how water is dissociated in the case of the Ni/K mixture. One possibility is that there is a very small amount (>2%) of metallic nickel dissolved in the NiO. The other possibility is the formation of a Ni(+3) species from potassium oxide, nickel oxide and water which can then oxidize carbon to CO₂ and H₂ while being reduced to NiO. At this time one cannot distinguish between these two potential mechanisms.

c) Adsorption and TPD Studies

In order to get a better chemical understanding of surface intermediates during gasification with CO, CO₂, O₂ or H₂O, a series of experiments on adsorption and temperature programmed desorption (TPD) were carried out on graphite. These are described in detail in Appendix B, which is a draft of a paper and of a Ph.D. thesis to be published. Three types of surface species are suggested after adsorption of CO, CO₂, H₂O and O₂ on graphite. A low temperature (100-400^oC) precursor is observed after CO adsorption and is likely due to weakly bound species such

as carbonyl and/or ether groups. The low desorption temperature of this species suggests that no graphitic carbon-carbon bonds are broken.

A high temperature CO precursor ($700-1000^{\circ}\text{C}$) is observed after adsorption of any of the four gases. It is assigned to a semi-quinone species. The desorption of this species involves breaking of two carbon-carbon bonds in the graphite lattice, explaining the high desorption temperature.

Formation of the high temperature CO precursor may be by reaction of an oxygen and a carbon atom in the cases of CO_2 , H_2O and O_2 adsorption. In the case of CO adsorption there is no dissociation and the precursor is formed by insertion of a molecule into the graphite lattice. This insertion requires a graphitic carbon-carbon bond breaking both, for the formation and desorption of the species. This is a highly activated process occurring only at high temperatures.

A low temperature ($200-600^{\circ}\text{C}$) CO_2 precursor is also observed after adsorption of all four gases. It is assigned to a lactone group. Formation of CO_2 from decomposition of a lactone group is analogous to decarboxylation reactions.

APPENDIX A

INVESTIGATION OF THE SURFACE SPECIES ON GRAPHITE
IMPREGNATED WITH POTASSIUM AND/OR NICKEL COMPOUNDS

1 RESULTS

1.1 Kinetic results

1.1.1 Catalyst derived from $\text{Ni}(\text{NO}_3)_2$ alone

If $\text{Ni}(\text{NO}_3)_2$ deposited on graphite is heat treated in Ar at 723K prior to the introduction of steam, no catalytic activity is observed at 893K for up to 2 hours. This catalyst is only active when it is pretreated under reducing environments, H_2 at 723K, or Ar at 923K, in which case carbon becomes the reducing agent. In this case the initial carbon consumption rate is equal to $2.0 \text{ mol C}/(\text{mol Ni} \times \text{min})$ with a ratio of CO/CO_2 equal to 0.22. The initial rate of carbon consumption is maintained for the first ten minutes, and it then decreases very rapidly (see figure 1). After 80 to 200 min, depending on the sample, the catalyst has completely deactivated. At this point a graphite conversion of $50 \pm 15\%$ has been reached, as determined by both carbon weight loss and total gas production.

After the catalyst has completely deactivated, its activity cannot be recovered by either treatments in reducing conditions (923K in Ar or

723K in H_2) or by a combination of oxidizing and reducing conditions (723K in O_2 and then 923K in Ar).

1.1.2 Catalyst derived from KHO alone

No steady rate steam gasification at 893K is observed when KOH is deposited on graphite. The same result is obtained when KNO_3 is used instead of KOH. If the sample is heated to 1073K, a rate of carbon consumption equal to $0.18 \text{ mol C}/(\text{mol K} \times \text{min})$ is observed, with a ratio of CO/CO_2 in the gas products equal to 0.15. Treatment in an O_2 atmosphere at 723K prior to the introduction of steam did not change this result.

1.1.3 Catalyst derived from a $KOH/Ni(NO_3)_2$ mixture

When the catalyst derived from a 1:1 molar mixture of KHO and $Ni(NO_3)_2$ loaded on graphite is treated in Ar at 723K and then exposed to water vapor at 893K, an initial carbon consumption rate of $2.5 \times 10^{-2} \text{ mol C}/(\text{mol Ni} \times \text{min})$ is observed with a CO/CO_2 ratio of 0.08 (figure 1). Over a period of 24 hours, the product distribution remains constant, and the reaction rate decreases by only 10%.

When the Ni/K catalyst is reduced in H_2 prior to the introduction of steam, an initial high carbon consumption rate is observed ($1.5 \text{ mol C}/(\text{mol Ni} \times \text{min})$), with a CO/CO_2 ratio equal to 0.33. Even though this rate is lower than that obtained with the catalyst derived from $Ni(NO_3)_2$ alone, and it starts to decrease sooner,

the Ni/K catalyst pre-reduced in H_2 does not deactivate completely as in the case of Ni alone (see figure 1). After 20 min, the reaction rate is similar to that obtained when the catalyst has not been pre-reduced, and from there on both cases show the same kinetic behavior. If the catalyst is treated again in H_2 at 943K after 10 hours in steam at 893K (point A in figure 1), no noticeable increase in the rate of carbon consumption is observed after the re-introduction of steam at 893K.

1.2 XPS results

1.2.1 Catalyst derived from $Ni(NO_3)_2$

Bulk NiO is formed after heat treatment of $Ni(NO_3)_2$ deposited alone on graphite at 723K in vacuum. Figure 2, curve (a) shows that after this treatment the $Ni2p_{3/2}$ adiabatic peak has a binding energy of 855.2eV, which is 1.4eV higher than that observed for Ni foil, and a satellite at 862.2eV, both typical of NiO. The adiabatic peak has a shoulder at higher binding energies possibly due to the addition of the multiplet splitting peak, typical of high spin Ni(II) species, and some surface $Ni(OH)_2$ [Kim 74]. The O 1s signal shows a peak at 530eV, typical of transition metal oxides, and a shoulder at 532eV, due to the presence of surface OH^- groups (figure 3)[Wandelt 82]. Nickel deposited on graphite that has been pre-treated in Ar at 723K remains as NiO when it is exposed to H_2O vapor for 10 min (see figure 2, curve (b)). Longer exposures (up to 135 min) in H_2O under the same conditions do not alter this result.

When $\text{Ni}(\text{NO}_3)_2$ deposited alone on graphite is heat treated in vacuum at 923K for 30 min, $\text{Ni}(+2)$ is partially reduced to the metallic state. A comparison of curves (a) in figures 2 and 4 shows that the position of the $\text{Ni}2p_{3/2}$ adiabatic peak has shifted to a lower binding energy (854.7eV), and the intensity of the multiplet and satellite peaks has decreased considerable. There is also a decrease in intensity of the $0\ 1s$ peak at 530eV, corresponding to a reduction of 60% of the $\text{Ni}(+2)$ to the metallic state. Further treatment of the sample at 923K in vacuum did not increase the percentage of metallic Ni in the sample.

When the sample is treated in 10Torr flow of H_2O at 893K for 10 min, after the heat treatment at 923K in vacuum, an almost complete reduction of the $\text{Ni}(+2)$ is observed (see figure 4, curve (b)). The binding energy of the $\text{Ni}\ 2p_{3/2}$ peak (853.8eV) is very close to that obtained for Ni foil, and the $0\ 1s$ signal is very small. If the H_2O treatment at 893K is continued for 80 more minutes, however, Ni reoxidizes the metal to NiO as observed in figure 4, curve (c). The binding energy of the $\text{Ni}\ 2p_{3/2}$ peak shifts to 855.4eV, and the reappearance of the $0\ 1s$ signal at 530eV is in evidence for the oxidation process.

After Ni is oxidized due to the H_2O vapor treatment, it cannot be reduced back to the metallic state by heat treatment in vacuum at 923K, as shown in figure 5, curve (a). Reduction of the NiO is possible by treatment in H_2 at 723K (figure 5, curve (b)), but exposure to H_2O vapor at 893K for 5 min after this treatment is enough to completely re-oxidize the nickel (curve (c) in figure 5).

1.2.2 Catalyst derived from KOH alone

Heat treatment at 723K; of a sample containing only KOH deposited on graphite favors the surface enrichment of potassium. The binding energy of the K $2p_{3/2}$ peak (294eV) is close to that reported for bulk KOH [Kishi 73]. From the ratio of intensities of the K $2p_{3/2}$ and C 1s signals, a ratio of potassium to carbon on the surface equal to 0.2 is determined, which is higher than the initial bulk concentration (K/C equal to 10^{-2}). The O 1s binding energy at 532eV, typical of a hydroxyl group, and the ratio of potassium to oxygen equal to 0.9, suggest the presence of multilayers of KOH on the graphite surface.

After treating this sample in 10Torr of H_2O at 893K for 10 min (figure 6, curve (c)), the potassium signal decreases drastically and the binding energy of the K $2p_{3/2}$ peak shifts to higher binding energies, compared with bulk KOH. The peak position varies from sample to sample and an average of 295.0 ± 1.0 eV was determined. The O 1s signal shows a peak at 534eV with a shoulder at 532eV.

If the sample is treated for 65 more minutes in H_2O , the K $2p_{3/2}$ signal completely disappears (see figure 6, curve (b)). Very similar results are obtained if KNO_3 is deposited on graphite instead of KOH.

1.2.3 Catalyst derived from a $Ni(NO_3)_2$ /KOH mixture

As in the case of the catalyst derived from $Ni(NO_3)_2$ alone, heat treatment at 723K in vacuum of a mixture of KOH and $Ni(NO_3)_2$

deposited on graphite favors the formation of NiO. The binding energy and lineshape of the Ni $2p_{3/2}$ signal obtained after this treatment for the nickel/potassium mixture is the same as that obtained after treatment of $Ni(NO_3)_2$ alone. The O 1s signal shows two peaks at 530 and 532eV. The peak at 530eV is associated with the presence of NiO, and the one at 532eV with the presence of multilayers of KOH on the carbon surface. As in the case of KOH deposited alone, heat treatment of the nickel-potassium mixture to 723K in vacuum favors the diffusion of KOH to the graphite surface. The K $2p_{3/2}$ binding energy is 293.8eV and the ratio of potassium to carbon is equal to 0.12, much higher than the initial bulk ratio (K/C equal to 10^{-2}).

When the sample is exposed to a 10Torr flow of H_2O at 893K for 15 min after the heat treatment at 723K in vacuum, the amount of potassium on the surface decreases substantially (curve (c) in figure 6). The K $2p_{3/2}$ binding energy in the case of the mixture remains at 283eV, in contrast to the shift to higher binding energy observed for the KOH alone (compare curves (a) and (c) in figure 6). In the case of the nickel-potassium mixture, the O 1s signal still shows two peaks at 530 and 532eV. The intensity of the 532eV peak decreases to a value such that the atomic ratio of potassium to oxygen remains equal to 1.0. The intensity of the 530eV peak remains constant, indicating that NiO is still present. This is corroborated by the Ni $2p_{3/2}$ binding energy (855.2eV), and lineshape (see figure 7, curve (a)).

Exposure to 10Torr continuous flow of H_2O vapor for 120 more minutes did not change either the oxidation state of nickel or the surface concentration of potassium. As mentioned previously, a similar

treatment in the case of KOH deposited was enough to completely suppress potassium from the carbon surface (compare curves (b) and (d) in figure 6).

When a fresh mixture of KOH and $\text{Ni}(\text{NO}_3)_2$ on graphite is treated in H_2 at 723K, complete reduction of the Ni(+2) and surface diffusion of KOH are observed, as in the case of the two components loaded by themselves on graphite. When the mixture is then treated in H_2O vapor at 893K for 5 min, partial oxidation of the Ni metal is observed (figure 7, curve (b)), and a 10 min treatment is enough for a complete oxidation. This result is the opposite to that observed for the catalyst derived from $\text{Ni}(\text{NO}_3)_2$ deposited alone, where after 10 min treatment in H_2O vapor at 893K, the surface concentration of potassium and binding energy of the K $2p_{3/2}$ peak is the same, regardless of whether the sample has been pre-reduced or not.

2. DISCUSSION

2.1 Catalyst derived from $\text{Ni}(\text{NO}_3)_2$ alone

The results obtained for the catalyst derived from $\text{Ni}(\text{NO}_3)_2$ alone are summarized in figure 8. These results show that, as also indicated by other authors, the activity of the nickel catalyst for graphite steam gasification can be associated with the presence of the metal under reaction conditions. After 10 min exposure to H_2O at 893K, figure 7 shows that the catalyst is active and figure 4, curve (b) shows that metallic nickel is present, whereas after 90 min, the catalyst has completely deactivated while figure 4, curve (c) shows that NiO has been

formed. The results also show that if the steam gasification reaction is carried out below 900K, a pre-reduction step is necessary in order to activate the nickel. That is, if metallic nickel is initially present (curve (a), figure 4), it can be stabilized under reaction conditions by its interaction with graphite (curve (b), figure 4), and the catalyst is active; but if the pretreatment is such that NiO is formed instead (curve (a), figure 2), then graphite is not able to reduce the oxide (curve 5, figure 2), and the catalyst shows no activity.

A mechanism for steam gasification of graphite by transition metals to form H₂ and CO₂ is described in equations (1) to (3), as proposed by several authors.



In this mechanism, below 900K, equation 2 cannot involve the direct reaction between NiO and graphite, as indicated by our XPS results. If this reaction were possible, the pre-reduction step just described should not be necessary, since the reaction represented by equation 2 would occur first, and then the metallic nickel would be oxidized by water, completing the cycle.

In order to justify the need of the preactivation step, equation 2 must involve the reaction of either an activated carbon or an activated oxygen species. In the first case, it is proposed that a surface carbide is involved in the gasification reaction. This species can be formed from the reaction between nickel metal and graphite, at their interface, then diffuse through the metal surface, and be removed by reaction with

oxygen formed from the dissociative chemisorption of H_2O . Various surface science studies indicate the feasibility of these steps at 900K (steam gasification reaction temperature). Also, the involvement of such species has been proposed in the literature for the platinum and iron catalyzed reactions. In the case of the nickel catalyst, ESR studies have suggested that a bulk carbide is not being formed during the gasification reaction. These results, however, do not discard the formation of a surface compound, since the technique used is only bulk sensitive.

Another possibility for the step represented by equation 2 is the reaction between oxygen chemisorbed on nickel metal and graphite. This has also been suggested for the iron catalyzed steam gasification above 100K. In this case, Ni metal serves as a site for dissociation of H_2O and recombination of H_2 . The chemisorbed oxygen then diffuses toward the nickel-carbon interface, reaction with graphite and forming, probably, the same type of CO precursor described in Appendix B., This precursor decomposes to give CO, which then reacts with H_2O (water-gas shift reaction) to produce CO_2 and H_2 .

These two models share some common points. In both cases Ni metal is the site for dissociation of H_2O , and it is required for the formation of an activated species. This species, then, has to diffuse across the nickel-carbon interface to form the oxygenated gas product.

Even though the presence of the metal correlates with the properties of the nickel catalyst, the formation of NiO cannot be considered as the cause of the loss of activity, but rather as another consequence of the deactivating process. The results in figure 5 show

that once the catalyst has deactivated and NiO is formed, Ni metal can be recovered by heating in H₂ at 723K. This treatment, however, does not regenerate the catalyst, and figure 5, curve (c) shows that exposure to H₂O vapor at 893K is enough to completely re-oxidize the metal. This is the opposite situation to that of a fresh sample where Ni metal is maintained after H₂O exposure at 893K.

Our results indicate that in the steam gasification of graphite, deactivation occurs when carbon is no longer able to stabilize nickel metal under reaction conditions. It is proposed that this occurs because there is a loss of contact between nickel and the edge planes of carbon, which hinders the diffusion of either surface oxygen or carbon species. This then prevents the removal of oxygen produced from the chemisorption of H₂O and allows the formation of NiO. The fact that graphite cannot reduce NiO at 973K in Ar in the case of the deactivated sample (figure 2, curve (a)), whereas this treatment is as efficient as the H₂ treatment in the case of the fresh sample, indicates that there is no intimate contact between the deactivated catalyst and the active planes of carbon.

A combination of several processes may be responsible for this total loss of carbon-nickel contact. Sintering of the nickel particles is certainly taking place under reaction conditions (893K in H₂O), as indicated by several authors. This process reduces the contact area between carbon and nickel, but does not explain, by itself, the total loss of contact. It is suggested that in addition to the sintering phenomenon, there is a decrease in the wetting properties of nickel on carbon, which causes the complete separation of the nickel particles from

the carbon edges. This can be caused by the presence of carbon in the nickel surface, as indicated for various other metals.

The reasons for the deactivation of the nickel catalyst varies with the chemical nature of the carbon substrate being gasified, as indicated by Lund. For the case of graphite gasification, he suggests that deactivation is caused by sintering, in agreement with our conclusion, and in the case of spherocarb, an amorphous carbon, he suggests that encapsulation of the metal particles by a graphitic layer is the cause of deactivation. XPS studies are an excellent way to distinguish between these two possible modes of deactivation because of its sensitivity to oxidation state and surface concentration of the catalyst. When catalyst encapsulation takes place, dissociative chemisorption of H_2O is hindered, therefore, metallic nickel should remain on the surface once the catalyst deactivates. This is the reverse of the situation described in this work for the case of graphite gasification where NiO is formed on the surface when the catalyst deactivates due to the loss of catalyst-carbon contact.

2.2 Catalyst derived from KOH alone

Under our reaction conditions (below 900K), KOH deposited alone is inactive for catalytic steam gasification of graphite. This result was also observed by Dellanay et al. on the same carbon substrate (graphite UCP-2). They suggested that KOH interacts with oxygen containing species in the carbon surface to form a surface compound that could only be thermally decomposed above 950K. These surface species have also been

proposed by other authors. Mims et al. suggested the formation of a "phenoxide" on the surface based on solid state NMR results, and Moulijn et al. suggested the formation of a similar species based on FTIR results, even though they raised questions about its involvement in the gasification process.

Our XPS results also suggest the interaction of potassium ions with oxygenated carbon surface species. This interaction is able to stabilize a small fraction of potassium on the surface under conditions in which bulk KOH would not be present. After treatment in 10 Torr H₂O at 893K for 10 min, a K 2p_{3/2} binding energy of 295±1eV was obtained. This value is higher than that observed for multilayers of KOH on graphite, even considering that its precision is not as good as those obtained for all the other cases. The higher potassium binding energy suggests that the potassium-oxygen bond has a larger ionic character than it has in KOH. This assumption is in agreement with the formation of a C-O^{-δ}K^{+δ} species, where the stabilization of the negative charge by the resonant π-system in graphite can be larger than by hydroxyl groups. After 10 min H₂O treatment at 893K, a potassium to carbon atomic ratio equal to 10⁻² was obtained and even though this is only a lower bound limit for the potassium surface concentration, due to the mean free path of the photoelectrons involved (15Å at 1000eV), it is safe to assume that it corresponds to a sub-monolayer coverage of K. Evidence for the formation of a potassium surface compound at submonolayer coverages has also been reported by Kelemen et al., based on UPS results.

After treatment in H₂O at 893K, the O 1s XPS signal shows a peak at 534eV, with a shoulder at 5332eV (figure 6, curve (c)). The 532eV

shoulder can be associated with hydroxyl groups, and the 534eV peak with carbon-oxygen surface groups. This is consistent with the assignment made by Kelemen et al. for adsorption of KOH on oxidized glassy carbon. In our case, from the intensities of the K 2p and O 1s at 532eV signals, a potassium to carbon atomic ratio higher than one would be obtained. This suggests either the formation of nonstoichiometric oxides, as proposed by several authors, or the interaction of some potassium ions with oxygenated species in the graphite surface, as also concluded from the K 2p analysis.

Even though some potassium ions can be stabilized on the carbon surface after treatment at 893K in H₂O vapor for 10 min, figure 6, curve (b) shows that after a similar treatment for 75 min, no potassium is observed. Our kinetic experiments, however, indicate that some potassium must be present at 1073K, since a catalytic rate of steam gasification is observed. The reason for this discrepancy might reside on the different H₂O partial pressures used in these experiments. In the XPS study, a continuous flow of 10Torr of H₂O vapor was used, while in the kinetic study the H₂O vapor pressure was above 760Torr. Since the H₂O sticking coefficient on carbon is extremely small, the concentration of oxygenated surface species under the kinetic conditions is higher than under the XPS conditions. Thus, in the former case a higher concentration of potassium ions can be stabilized, making possible the high temperature catalytic activity of KOH alone. Kelemen et al. have reported, based on AES results, that a much higher concentration of potassium ions can be stabilized on the surface of glassy carbon when the substrate is oxidized prior to the potassium deposition, which is consistent with our assumption.

2.3 Catalyst derived from a KOH/Ni(NO₃)₂ mixture

A summary of the results obtained with the catalyst derived from a mixture of KOH and Ni(NO₃)₂ is given in figure 9. These results indicate that the properties of the mixture are different from those of the components alone. The same conclusion has been reached previously, based on CAEM results and on kinetic results on both graphite and char gasification. Other authors have also reported similar situations for other transition metal-alkali mixtures such as nickel-calcium, iron-sodium and iron-potassium.

From the results presented in this section, three important differences are observed. The kinetic results show that the mixture is active after treatments under which the catalyst derived from Ni(NO₃)₂ alone is inactive. In the case of the mixture, the XPS results indicate that both KOH and NiO are stabilized on the surface under reaction conditions, whereas the potassium signal completely vanishes in the case of KOH alone, and Ni metal is present when in the case of the catalyst derived from Ni(NO₃)₂ alone. These results are explained by a strong interaction between nickel and potassium, probably of a chemical nature.

As reported in this and previous work, the main property of the nickel potassium mixture is the conservation of its initial activity for long periods of time. This is certainly related to the fact that the catalyst remains in contact with the active planes of graphite as observed in the CAEM study. The CAEM study also shows that the catalyst intrinsic activity is uniform among all the active areas in the carbon.

These results indicate that the nickel and the potassium are uniformly distributed within the catalyst and that its mobility is very high, such as in the case of a liquid phase. The use of alkali metal salts to decrease the melting point of high temperature oxides is a very common procedure. The interaction between potassium and nickel can lower the high melting point of NiO by formation of a eutectic compound, which is either the active catalyst or becomes a precursor for its formation. Similar results have been reported for the $K_2SO_4/FeSO_4$ mixture, and a similar conclusion has been reached.

The formation of such a compound can also explain the stability of potassium ion on the surface under conditions at which KOH is not present. Our results suggest that potassium is stabilized by interaction with nickel and not by its interaction with oxygenated groups in the carbon surface. If the latter were the case, a shift in the K 2p XPS signal to higher binding energies and a higher intensity O 1s peak at 534eV would be expected as in the case of KOH alone. Neither result is observed. Also, the high catalyst mobility of the nickel-potassium mixture suggests that the mixture is not "anchored" to the carbon surface by interaction with oxygenated surface groups.

An important difference between the catalyst derived from $Ni(NO_3)_2$ alone and the one derived from the $Ni(NO_3)_2/KOH$ mixture is that the former is only active when the metal is present, while the latter is active in conditions where $Ni(2+)$ is the major species. Furthermore, when both catalysts are simultaneously present, the gasification rates obtained can be accounted for by the addition of

the activities of the two catalysts. When a catalyst derived from a $\text{Ni}(\text{NO}_3)_2/\text{KOH}$ mixture is prereduced in H_2 , the gasification activity observed can be ascribed to a combination of an initial high activity that ends after 10 min, which is due to the fraction of free nickel present, and a lower but stable activity due to the nickel-potassium mixture. Again the formation of a nickel-potassium mixed oxide can justify the interaction of potassium with just a fraction of the nickel and be responsible for the different catalytic behavior when compared with the nickel catalyst alone.

An important point to be discussed is whether in the nickel-potassium mixture the activity is due to a small fraction of nickel present in the metallic state, and maintained active by the presence of potassium, or if the $\text{Ni}(2+)$ is directly involved in the gasification reaction. Our results cannot clearly distinguish between these two possibilities, but we would like to summarize the arguments in favor of each case.

a): The first possibility is that the active catalyst is a small amount of metallic Ni. The kinetic results presented in a previous section show that the product distribution and activation energies observed with the nickel-potassium mixture are very similar to those obtained with nickel alone, even though the gas production rates obtained with the mixture are lower. The CAEM study shows that the intrinsic activity of the nickel-potassium mixture is similar to that reported for Ni metal, but figure 1 shows that the initial bulk activity of the mixture is 50 times lower than that obtained with nickel alone. All these results can be justified by the formation of a very small amount of metallic Ni (~2%) that remains active due to the presence of

potassium. Such a small amount of Ni metal cannot be discerned by XPS in the presence of the oxide, therefore, its presence cannot be excluded. As previously discussed, potassium can be stabilized by its interaction with NiO, but the species formed is not the active one but rather a convenient support for the active Ni metal. This support can increase the mobility of the Ni metal and prevent the loss of contact with the carbon, which is the reason described for deactivation of nickel alone.

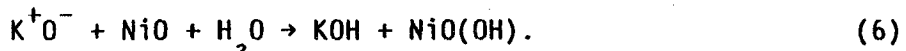
One important problem with this model is the question why the prereduction step is not necessary if the active species is Ni metal. A possible reason is that potassium, beside stabilizing NiO, also interacts with graphite and donates electron density to the valence levels of carbon increasing its reducing power. Evidence for the potassium-carbon interaction has been reported by Kelemen et al., based on UPS results, and it is implied by our XPS results as previously discussed. The effects of potassium on nickel and carbon are opposite since one would stabilize NiO and the other favor the formation of Ni metal. This might explain why only a small fraction of the nickel is stable as a metal. It has been reported earlier that mixtures of NiO and various alkali salts are more efficient than analogous mixtures with alkaline earth salts. This trend has also been reported by other authors and can be explained by the larger electron donation effects of alkalis compared with alkaline earths.

b): An explanation for the catalytic properties of the nickel-potassium mixture, without involving Ni metal as an active species, is also possible. NiO by itself is not active for steam gasification of carbon because it is not able to dissociate H₂O. The interaction of NiO with KOH, however, can create an active species for

dissociation of H_2O without involving the metal. It has been reported that alkali metal salts are able to stabilize O^- species. This species, as described in the literature, can be created by reaction of two adjacent KOH groups according to equation 5



The K^+O^- species can abstract a hydrogen atom from H_2O and induce its dissociation on the catalyst surface. The OH^- group attaches to the nickel atom and leads to the formation of a formal Ni(3+) species according to equation 6



It has been reported that NiO(OH) can be formed under oxidizing environments in the presence of alkali metal salts, and electrochemical studies show that oxidation of Ni(2+) to Ni(3+) depends on the concentration and kind of alkali metal hydroxide present.

This Ni(3+) species has a strong oxidizing power and can react with carbon (equation 7) to produce CO_2 and regenerate the Ni(2+) species, completing the cycle.



Even though the two mechanisms are quite different they have common points. In both cases the interaction between nickel and potassium creates a new species which gives the system catalytic properties that are not present with either component alone. In the first possibility described, this species is not the active one but maintains Ni metal active, whereas in the second case this species is the actual active site for dissociation of H_2O . It is clear that more evidence is necessary to support or reject either mechanism, but the idea we want to emphasize

at this point is that the mixture of a transition metal and an alkali metal can generate catalysts with particular properties for steam gasification of carbon solids that are better than those of the components alone. The same conclusions have been reached by several other authors for the gasification of a variety of carbon substrates and with various kinds of transition metal-alkali mixtures.

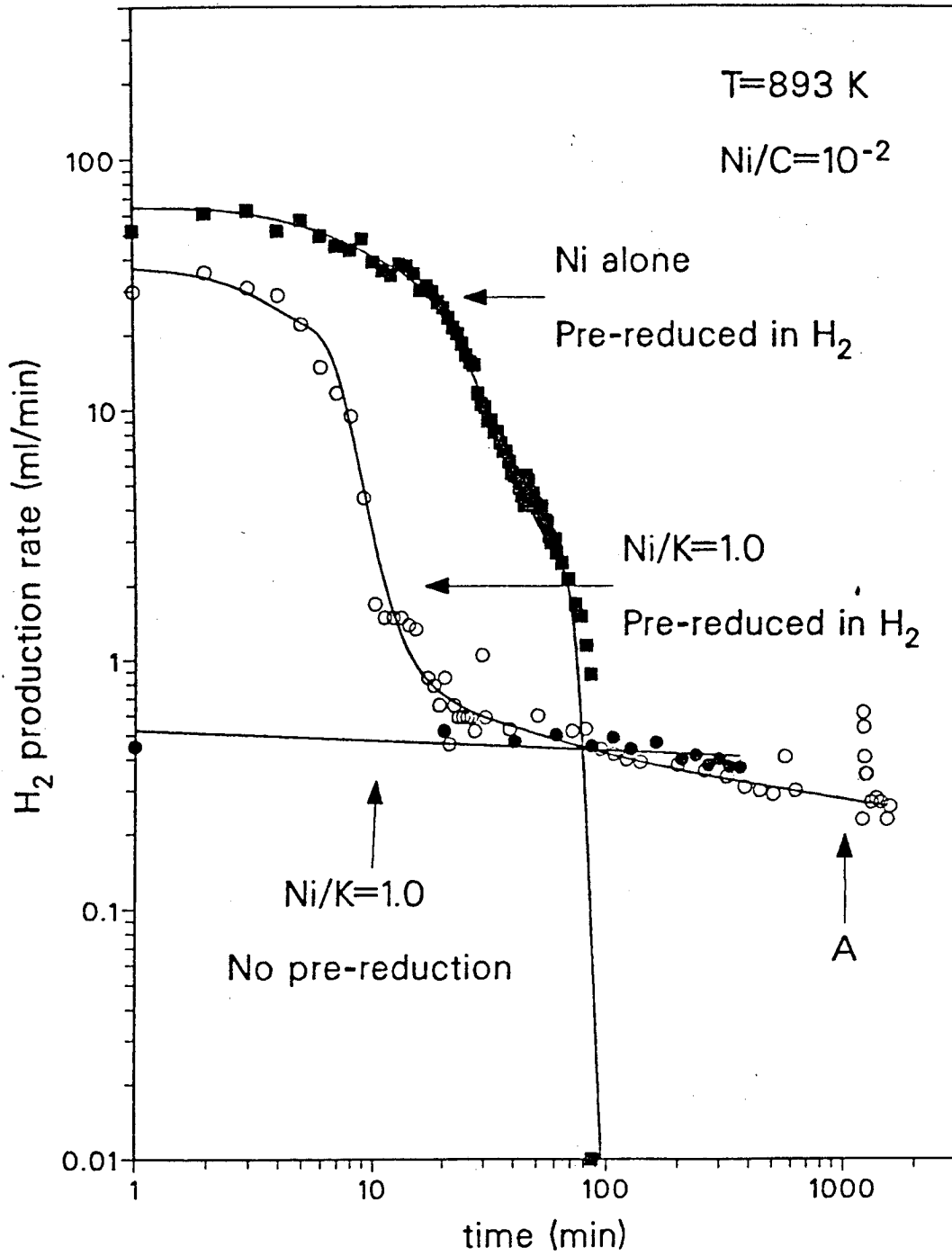


Figure 1

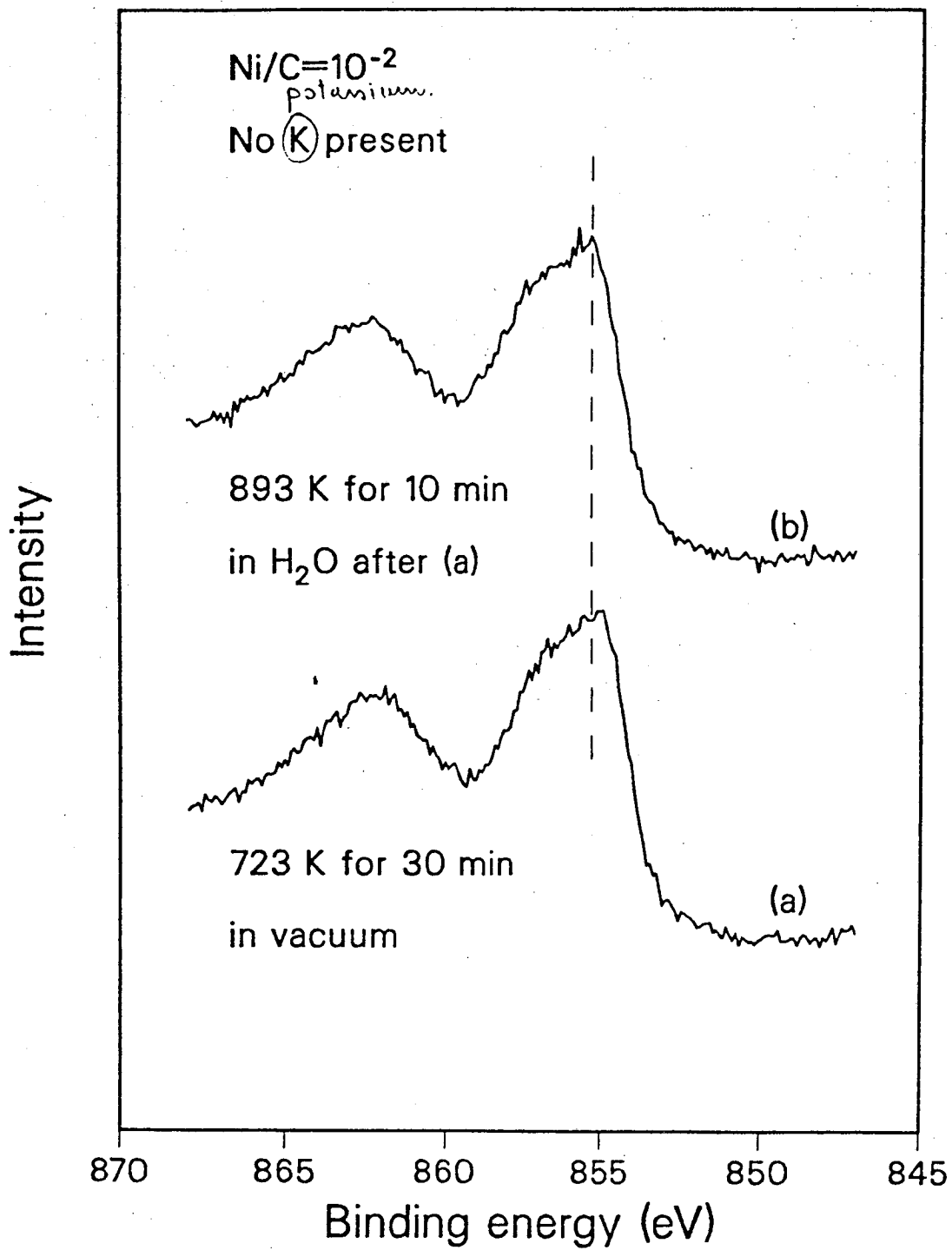


Figure 2

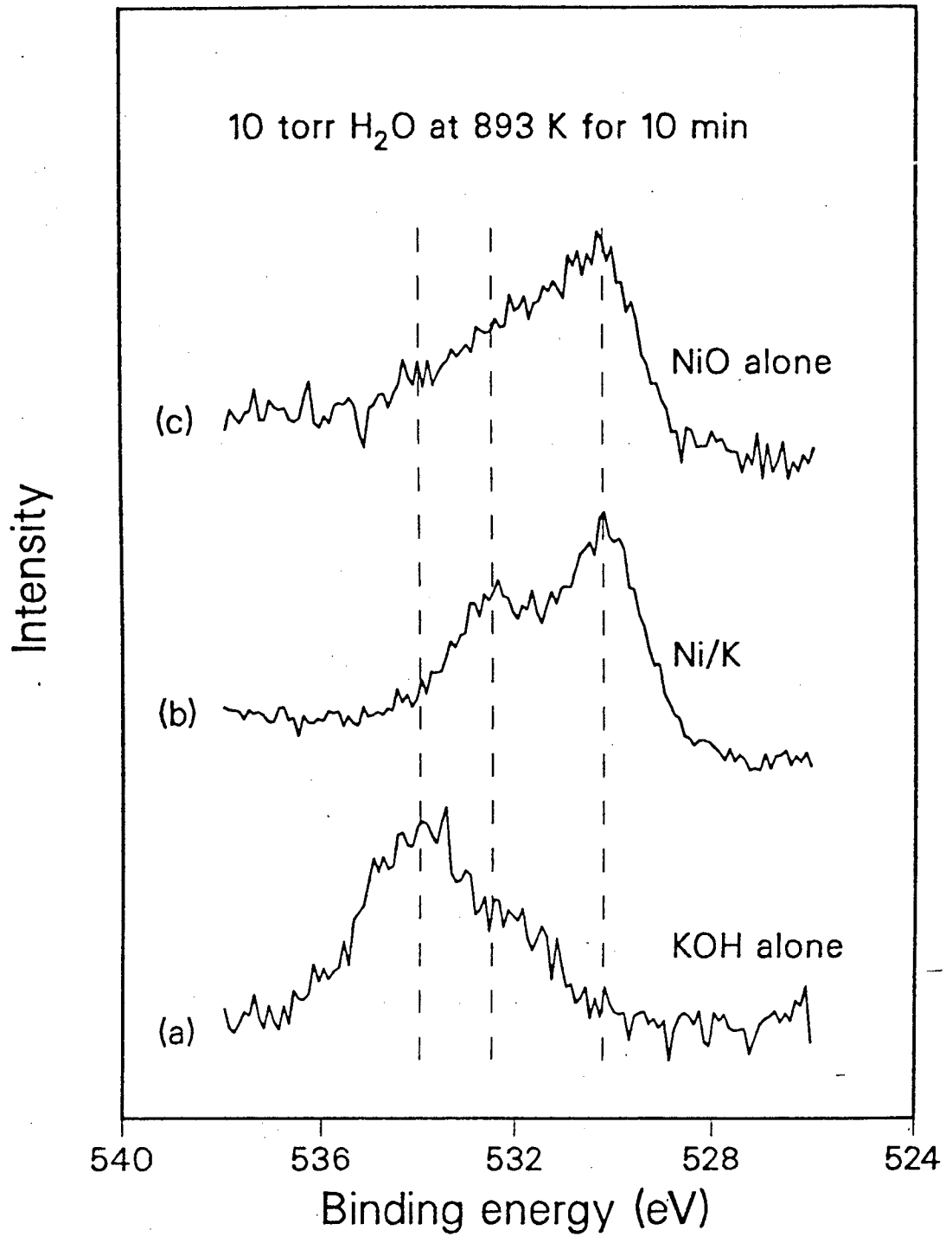


Figure 3

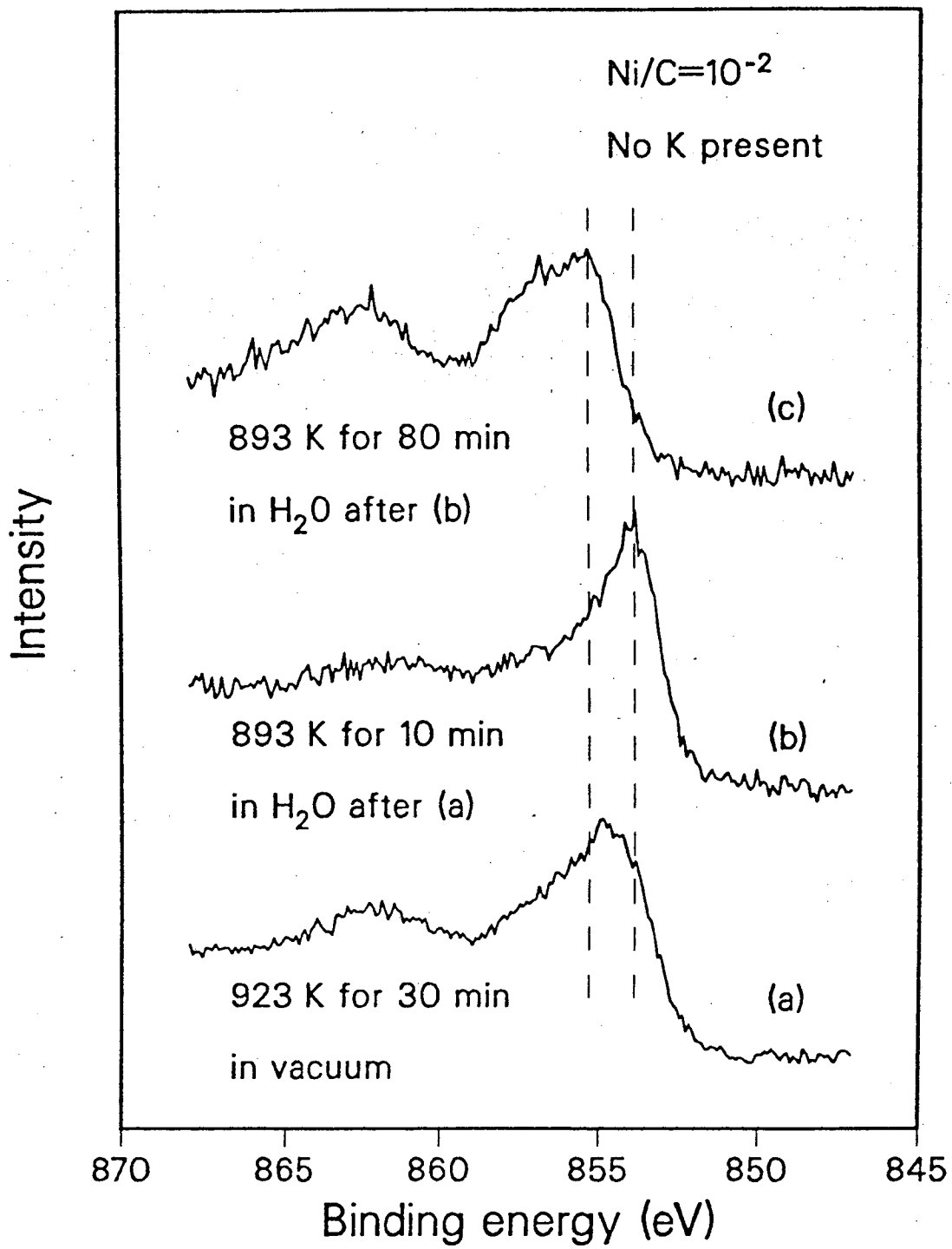


Figure 4

Treatment^s after 893 K in H₂O for 90 min

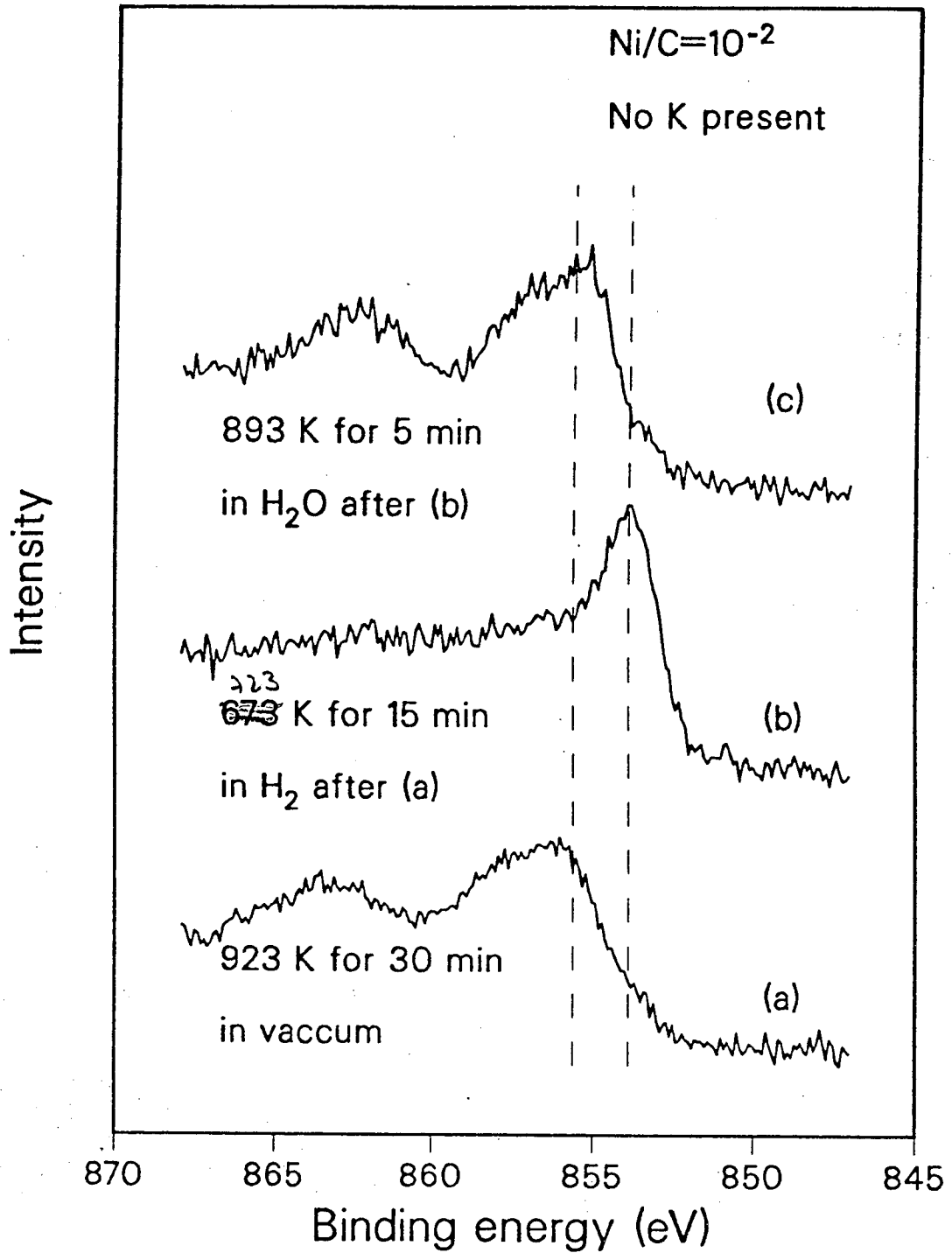


Figure 5

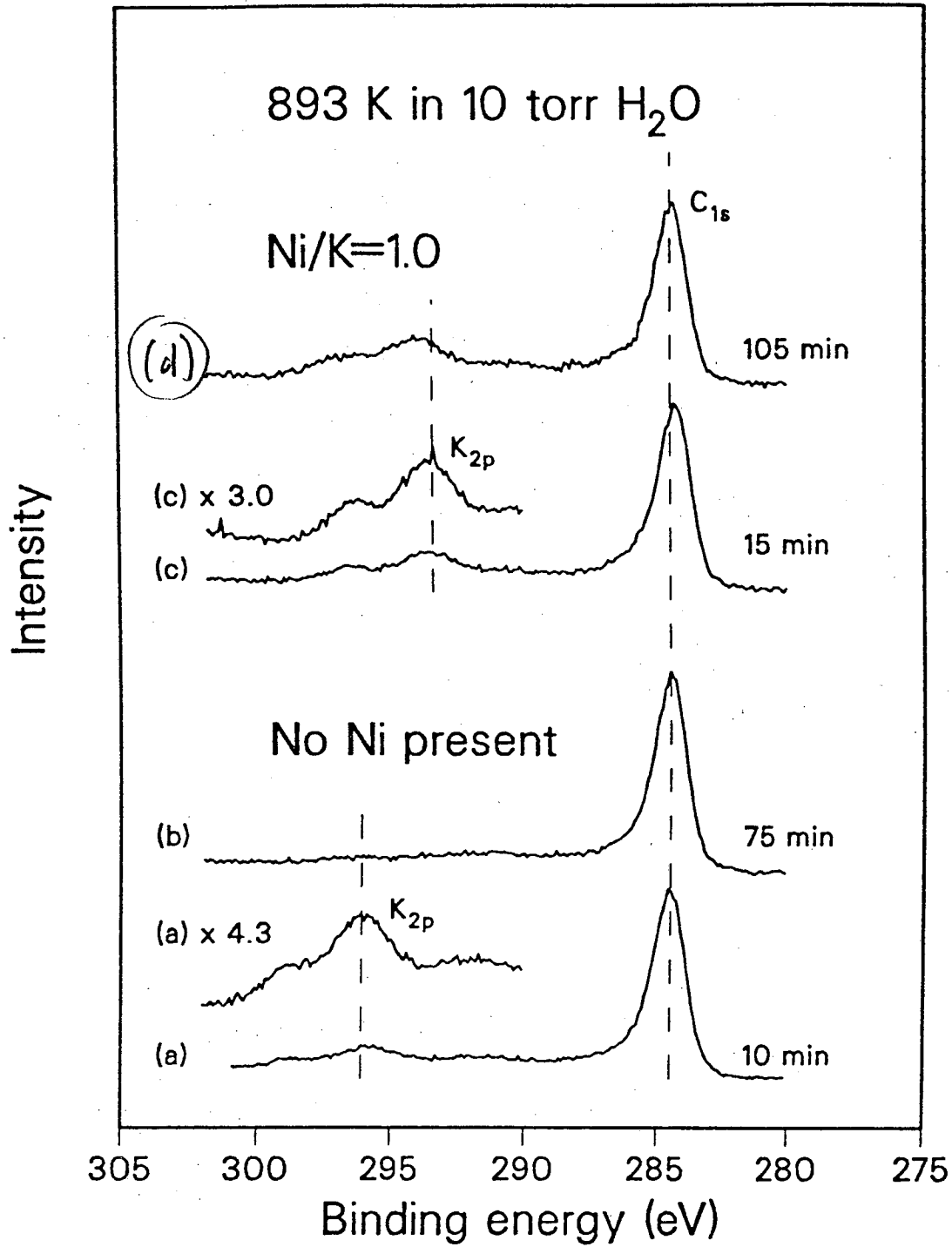


Figure 6

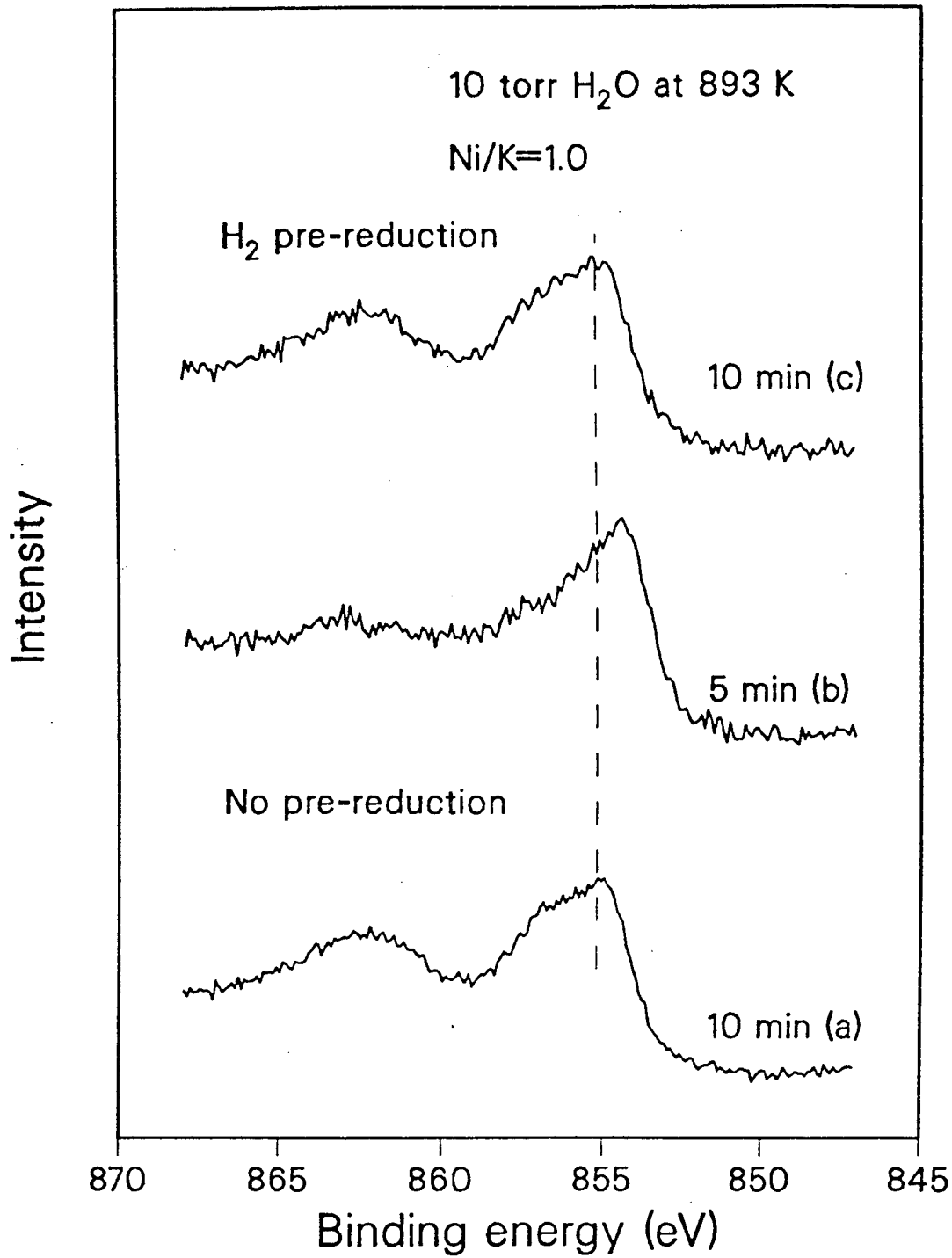


Figure 7

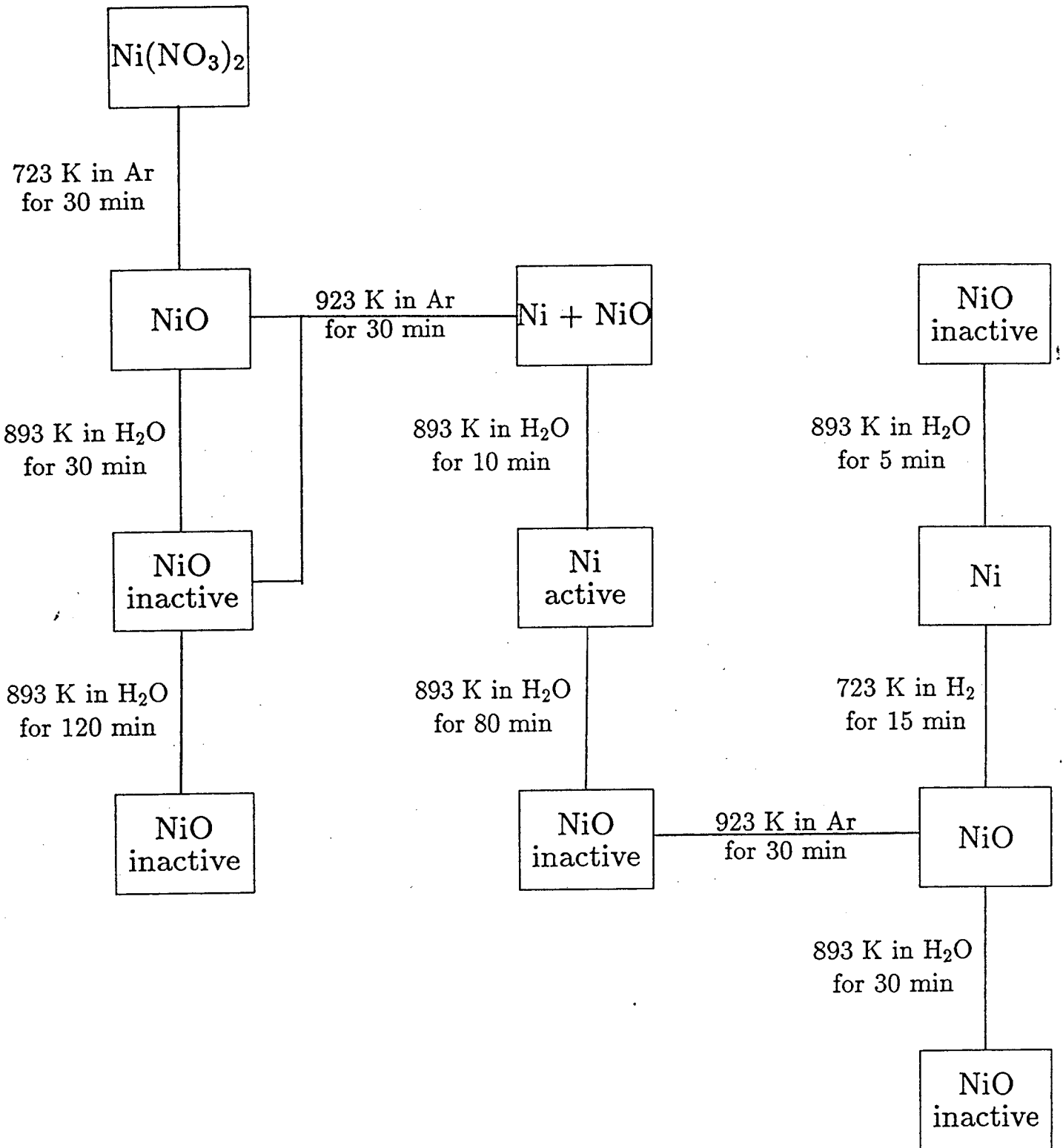


Figure 8

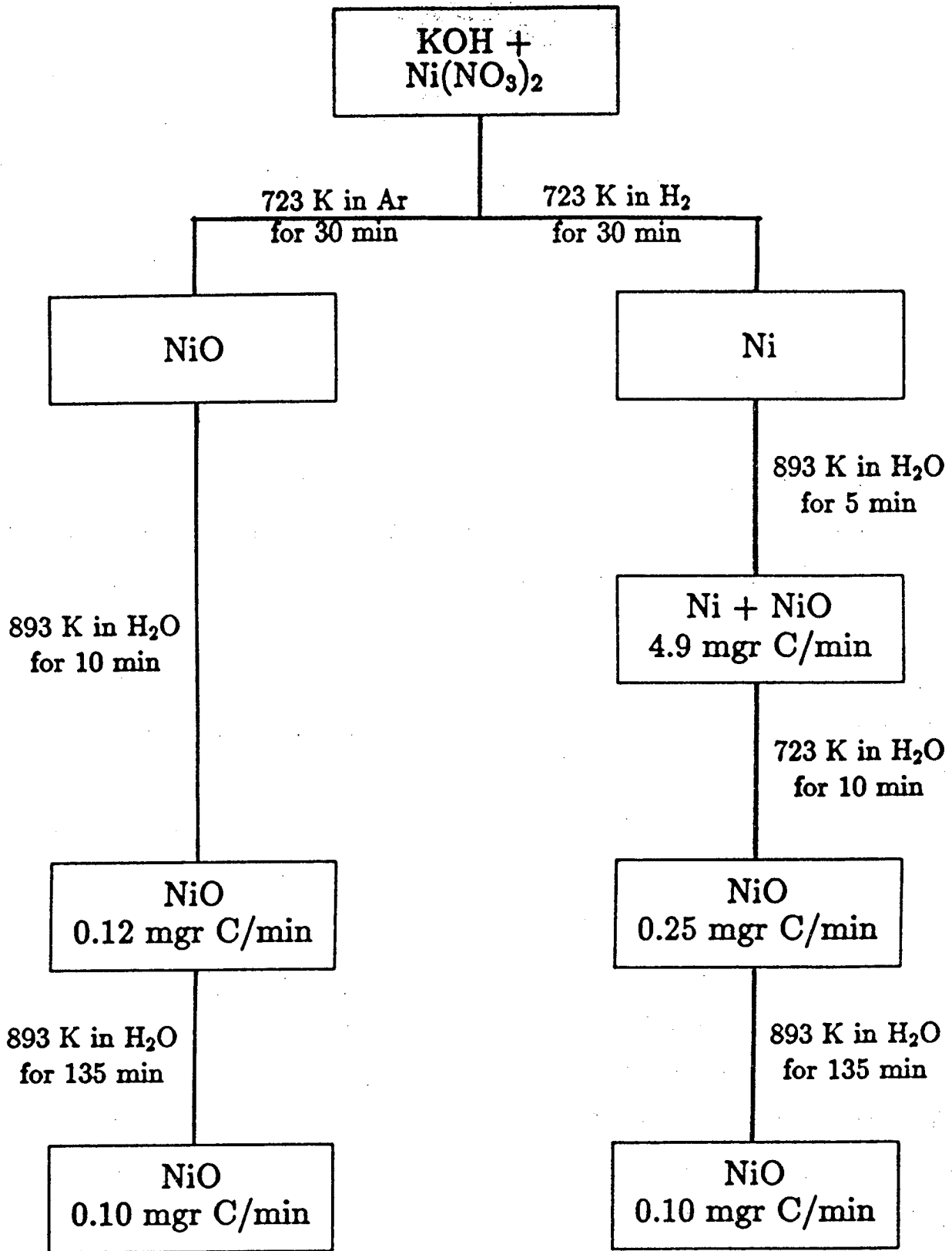


Figure 9

APPENDIX B

ADSORPTION OF CARBON MONOXIDE, CARBON DIOXIDE,
OXYGEN AND WATER ON CLEAN GRAPHITE

1. INTRODUCTION

Knowledge of the type and stability of the various surface species formed after adsorption of CO, CO₂, O₂ and H₂O on graphite are very important for the understanding of graphite chemistry and its implication on processes such as carbon gasification.

No work has been published on the adsorption of CO on graphite, and in the case of CO₂, O₂, and H₂O adsorption, even though numerous studies have been reported, little understanding has yet been achieved, owing to the complexity of the system. Studies have been conducted on various carbonaceous samples like graphite, carbon black, glassy carbon, coconut char and carbon fibers. Techniques such as gravimetric balances [1-5], reactor beds [6], pH measurements [7,8], Auger electron spectroscopy (AES)[9,10], infrared adsorption [11-14], X-ray photoelectron spectroscopy (XPS)[15-17], ultra-violet photoelectron spectroscopy (UPS)[18], electron-spin resonance (ESR)[19], transmission electron microscopy (TEM)[20], and temperature programmed desorption (TPD)[21-28] were employed and brought some useful information about the nature of the graphite species. In particular, TPD and XPS

have proven to be good probes for the study of surface adsorbates, but in the case of carbon-oxygen species, the work has been conducted mostly on raw, or highly oxidized carbon samples under not very well controlled atmospheres, giving broad features, difficult to analyze.

The approach of this work has been to study species produced by the chemisorption of CO, CO₂, O₂ and H₂O, and their isotopic derivatives onto a clean graphite sample, and under ultra high vacuum (UHV) conditions. This procedure allowed to cover only a small amount of the sites on the surface, giving much better resolved and reproducible TPD features. Also, XPS studies have been carried out in order to determine surface concentration of the adsorbed gases, and to attempt to assign the TPD features to plausible species on the graphite surface.

Experiments have been carried out on graphite samples from three different origins to check the reproducibility of the results. Kinetic measurements have also been undertaken to study the interconversion of CO and CO₂ at the graphite surface (Boudouard equilibrium).

2. RESULTS

2.1 CO Adsorption

The CO adsorption kinetics are presented in figure A. The total CO desorption, measured by integration of the mass 28amu TPD peak, is plotted versus exposure at various pressures.

The thermal desorption spectra taken after adsorption of 6×10^{-5} Torr of CO for 30s at different temperatures is plotted in

figure B. When adsorbed at 50⁰C, CO desorption occurs in two overlapping peaks at 120 and 230⁰C, and when adsorption is carried out at higher temperatures, peaks at 400, 700 and 820⁰C are also obtained. No ¹²CO is evolved after adsorption of ¹³CO, showing that no carbon exchange with the bulk occurs. This allows also to rule out any contamination from O₂ or H₂O, since they would lead to ¹²CO desorption. Additional experiments performed with C¹⁸O confirm this observation.

Some CO₂ (mass 44amu) is also produced after CO adsorption (figure C). Room temperature adsorption leads to a single peak at 170⁰C, whereas higher adsorption temperatures lead to more stable species that desorb at 400 and 650⁰C. In our experimental conditions the amount of CO₂ desorbed after CO adsorption is always less than 10% of the total amount of CO chemisorbed.

2.2 CO₂ Adsorption

The TPD spectra for mass28(¹²CO), 29(¹³CO), 44(¹²CO₂) and 45amu(¹³CO₂) after exposure to 8Torr of ¹³CO₂ for 60s are reproduced in figure D. Molecular ¹³CO₂ desorbs at 150⁰C. A large high temperature ¹²CO TPD peak at 820⁰C is observed, with two shoulders at 700 and 980⁰C. C¹⁸O₂ adsorption results in identical desorption peaks at mass 30amu (C¹⁸O) indicating that these high temperature features are not due to contaminants. Some ¹³CO (mass 29amu) is evolved at low temperatures, and a weak mass 44amu signal (¹²CO₂) can be ascribed to isotopic impurities.

Adsorption of a 58-42% mixture of $C^{16}O_2$ and $C^{18}O_2$ leads to nearly total oxygen scrambling of the CO_2 desorbed, as 35% $C^{16}O_2$ (mass 44amu), 41% $C^{16}O^{18}O$ (mass 46amu) and 24% $C^{18}O_2$ (mass 48amu) is evolved (figure E). Theoretical proportions for the total scrambling are 34, 48 and 18% respectively.

Under UHV conditions, CO_2 chemisorption leads to the same TPD features as after adsorption at high pressures. Again, the 28amu TPD signal shows a maximum at $820^{\circ}C$, which can be enhanced by raising the adsorption temperature (figure F). A shoulder near $950^{\circ}C$ becomes the predominant feature of the spectrum, when adsorption is carried out at $700^{\circ}C$. Finally, the $700^{\circ}C$ shoulder observed after high pressure exposure or after O_2 adsorption is hardly detectable.

2.3 CO and CO_2 Interconversion. Kinetic Study

Reaction rates for CO and CO_2 reactions with graphite were obtained using the high pressure cell reactor. Data for the $C + CO_2 \rightarrow 2 CO$ reaction as a function of temperature (plotted in Arrhenius form) is shown in figure G. The reaction rates were calculated assuming a surface site concentration of $5 \times 10^{14} cm^{-2}$. The slope of this line yields an activation energy of $67 \pm 3 kcal/mol$. This value is in agreement with that obtained in flow reactor experiments ($59 kcal/mol$)[29].

Figure H shows a similar plot for the reverse reaction, $2 CO \rightarrow C + CO_2$. In this case, rates were measured from the accumulation of CO_2 , and the linear portion of the curve yields an activation energy for CO_2 formation of $24 \pm 2 kcal/mol$.

2.4 O₂ Adsorption

Figure I shows the TPD spectra of mass 28amu obtained after exposing the clean surface to various doses of O₂ at 250°C. Two maxima at 820 and 980°C, and a shoulder at 700°C are observed. High exposures are necessary to get a measurable adsorption signal. O₂ chemisorption can be enhanced by raising the adsorption temperature (figure J), with the 820°C TPD peak increasing the most. Some CO₂ (mass 44amu) is also evolved. Figure K shows two maxima at ca. 190 and 420°C, and a tail around 600°C. The intensities are expanded by a factor of 20 compared to figures I and J. Raising the adsorption temperature allows the observation of at least three other peaks at 300, 520 and 650°C, so that a total of five different chemisorbed species yielding CO₂ are isolated (figure H). The adsorption of a mixture of 47% ¹⁸O₂ and 53% ¹⁶O₂ produces TPD features of masses 44amu (C¹⁶O₂), 46amu (C¹⁶O¹⁸O) and 48amu (C¹⁸O₂) (figure M). Like for CO₂ adsorption, total scrambling occurs, since the intensities for the mass 44amu, 46amu and 48amu signals are 33, 19 and 48% for the 160°C peak, and 31, 24 and 45% for the 420°C peak, as shown in figure M. The theoretical values for total isotope mixing are 28, 22 and 50% respectively. Similar isotopic ratios were measured for the other TPD features at 300, 520 and 630°C, and are not reproduced here.

The O_{1s} XPS signal after extensive O₂ exposure (250Torr O₂ for 5 min at 530°C) is shown in figure N curve A. The peak is centered around 532eV, and it is similar to that obtained after CO chemisorption, although more intense. No difference in the C_{1s}

signal is observed after this treatment, compared with clean graphite. In agreement with the TPD results (figure I), oxygen on the surface desorbs thermally and the clean surface is recovered after flashing the graphite sample to 1080°C, as shown by the decrease in the O₁₅ signal (curves B to D in figure N). Variations in the position of the maximum with flashing temperature are within experimental error.

2.5 H₂O Adsorption

Under similar conditions, adsorption of H₂O on clean graphite is much lower than for O₂ and CO₂ adsorption. Exposures to high H₂O pressures (> 1Torr) are necessary to detect the desorption products in TPD experiments. The TPD signal at mass 2, 44 and 28amu, corresponding to the desorption of H₂, CO₂ and CO after exposure to 20Torr of H₂O for 60s are reproduced in figure O. H₂ is evolved at high temperatures (ca. 1000°C). CO₂ desorbs in a broad peak at temperatures between 100 and 500°C. CO shows the usual massif centered around 820°C, with a shoulder at lower temperatures, and a small peak near 1000°C. Two other peaks at mass 28amu and around 200 and 400°C are also observed. These peaks are not present after O₂ or CO₂ chemisorption, and are likely to be C₂ hydrocarbons. Other hydrocarbons are also produced. Figure P shows the TPD spectra taken after H₂O adsorption (20Torr for 670s), for masses corresponding to C₁ (15amu), C₂ (26-30amu), C₃ (39-41amu) and C₆ (78amu) hydrocarbons. The scale in figure P is expanded by a factor of 10 compared with figure O.

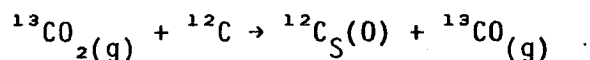
The integrated intensity of the H_2 peak is slightly less than one-third of the total CO produced, while the low temperature CO_2 massif, not well resolved, corresponds to less than one-tenth of the total CO signal.

In order to increase the total amount of H_2O adsorbed, physical wetting of the clean graphite was carried out. The utilized procedure is described in the experimental chapter. In figure Q the O_{1S} signal of the wetted surface is reproduced, and compared to the one after exposure to 20Torr of H_2O vapor for 60s. It is immediately apparent that the wetted surface contains much more oxygen than the one exposed only to H_2O vapor. The binding energy of the O_{1S} signal after H_2O wetting (533eV) is higher than that observed after O_2 chemisorption (532eV). The C_{1S} XPS single shows, after physical wetting, a tail located in the higher binding energy region (figure R). The difference between the signals from the wetted and clean samples shows a maximum at, ca. 287eV, 2eV higher than the peak position for the graphite signal. This shift is characteristic of weakly oxidized carbon atoms [16]. The integrated intensity of this difference is about 20% of that from the clean surface. The thermal decomposition of the wetted surface occurs at $350^\circ C$ (figure S), and the decomposition product is mostly H_2O , as observed by TPD. After flash at $390^\circ C$, the O_{1S} signal weakens considerably, and shifts to 532eV. This signal is, however, still larger than that observed after exposure to 20Torr H_2O vapor. The signal vanishes after heat treatment above $700^\circ C$ (figure Q).

3 DISCUSSION

Figure T shows that CO desorbs in two temperature regions after CO adsorption. When CO is adsorbed at room temperature, desorption peaks at 120, 230 and 400⁰C are observed, and when CO is adsorbed above 500⁰C, TPD peaks at 700 and 820⁰C are obtained. These results suggest that the two temperature regions are due to the desorption of two distinct surface species. The high temperature species is also observed after CO₂, O₂ and H₂O adsorption (figures E, K and O), and even though the CO low temperature species have not been reported after adsorption of other gases on graphite, desorption of CO from metal surfaces usually occurs in this temperature region (100-400⁰C)[30]. When ¹³CO is adsorbed on clean graphite, no ¹²CO is produced at high temperatures. This indicates that, even though the CO interacts strongly with the graphite surface, it does not dissociate .

Figure G shows that the major desorption product after CO₂ adsorption is CO at high temperatures. This figure also shows that the adsorption of ¹³CO₂ favors the desorption of ¹²CO, indicating the dissociation of CO₂, and the incorporation of one oxygen atom in the carbon lattice, to describe ¹²C_S(O) at high temperatures. This agrees with the mechanism proposed earlier by several authors [6,28,31].



where the ¹²C_S(O) species is likely to be the same high temperature species obtained after CO adsorption. The above reaction implies the release of ¹³CO, which can further adsorb on the surface. This is a very low probability process, as later discussed, and for this reason the

area of the mass 29amu peak in figure E is much lower than that of the mass 28amu peak.

The O_{1s} signal after O_2 and CO adsorption shows a maximum at a binding energy of 532eV (figure N). This suggests, as in the case of the TPD results, that similar surface species are formed after adsorption of these gases. The peak position at 532eV is lower than that reported for covalent non-polarized oxygen bonds (534eV), and higher than that reported for compounds containing O^- (531eV)[32], suggesting the formation of a polarized carbon-oxygen covalent bond.

CO_2 (mass 44amu) is also produced after adsorption of O_2 , H_2O , CO_2 and CO (figures C, D, K and O) although in smaller amounts than CO. Whereas only three desorption peaks at 170, 400 and 650°C are observed after CO adsorption (figure C), five peaks can be resolved after O_2 adsorption, at 190, 300, 420, 520 and 630°C (figure H). These various peaks are attributed to the desorption of the same type of species from different chemisorption sites. TPD after H_2O exposure does not show such well resolved peaks. Instead, a broad continuum from 100 to 500°C is observed (figure O), which is likely to originate from the same kind of species.

After O_2 and CO_2 chemisorption, complete oxygen scrambling is observed in the CO_2 desorbed, as indicated by isotope experiments (figures E and M). This indicates that in both cases CO_2 is produced from the interaction of two adsorbed molecules. A possible mechanism for the formation of CO_2 is given later in the discussion.

Assuming a frequency factor of $10^{13}s^{-1}$, Redhead's equation [33] can be used to estimate the desorption energies from the peak

temperatures in a TPD experiment. The values obtained for the CO and CO₂ species observed are summarized in Table 1. A comparison between these values and the activation energies obtained in kinetic experiments for CO₂ gasification and the Boudouard reaction indicates that both reactions are controlled by the desorption of the products. The activation energy for CO₂ gasification (67kcal/mol) agrees very well with the desorption temperature for CO formation after CO₂ exposure (64kcal/mol), and the activation energy for the Boudouard reaction (24kcal/mol) coincides with the lower limit in activation energy for desorption of CO₂ after CO adsorption (28kcal/mol).

TPD experiments after H₂O adsorption show that H₂ is evolved at very high temperatures (ca. 1000⁰C), in agreement with results obtained by Matsumura et al.[27]. From the integrated intensities, the amount of H₂ evolved accounts for less than one-third of the total CO produced, whereas the hydrogen from the desorbing hydrocarbons is one order of magnitude less than the H₂ evolved. A reason for the lack of mass balance in the TPD products is that after H₂O chemisorption the two hydrogen atoms produced can either recombine and form H₂, or form carbon-hydrogen bonds on the surface, which then decompose around 1000⁰C.

Since hydrocarbon evolution after H₂O exposure occurs between 100 and 400⁰C, it probably only involves breaking of carbon-carbon single bonds, rather than much more stable aromatic bonds. To account for such behavior, the existence of aliphatic fragments such as -CH₂-, -CH₃, or even -C₂H₅ functionalities must be proposed. Their thermal decomposition

would lead to radical formation, which would yield hydrocarbon molecules after recombination. The origin of the two maxima around 200 and 400°C (figure P) remains unexplained.

As mentioned in the introduction, there has been a great number of studies on the surface oxides adsorbed on carbon. Based on spectroscopy methods, these studies have proposed the existence of various types of surface groups. Our results imply that some of these species are present on the graphite surface after CO, CO₂, O₂ and H₂O. It would be interesting, then, to assign the various TPD features obtained in this work to plausible surface species. As previously mentioned, analysis of TPD data provides information about the desorption energy of the surface species involved, which is related to the strength of the bonds involved in the desorption process. By comparing these values with bond energies in similar organic compounds, tentative assignments of the various desorption features to surface species can be made.

It should be noticed, however, that it is difficult to get precise values of the bond energies on the graphite surface, from desorption energies obtained from TPD. First, desorption energies are the sum of the activation energies for desorption and the surface bond energy. This activation energy is very low in the case of CO desorption from metal surfaces [30], but it is known to be of the order of 10kcal/mol [4] or greater [9] for O₂ adsorption on graphite. In addition, Sanderson has pointed out [34] that the reorganizational energy of radicals after breaking the surface bond is an important contribution to the desorption energy, and in the graphite case this energy is expected to be considerable because of electron delocalization. Another complication to the determination of the bond strengths from TPD experiments is that the

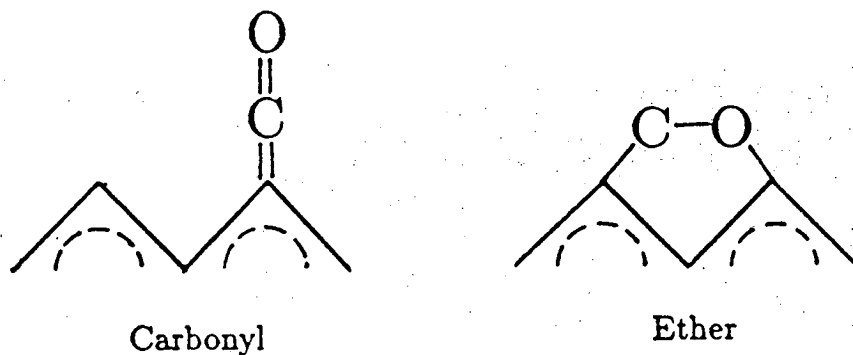
edges of the graphite particles contain various adsorption sites that lead to species of different stability whose desorption will broaden the TPD features [12]. For example, theoretical calculations [35] have shown that arm-chair sites are less reactive than zig-zag sites but give more stable species after adsorption. It is thus expected that TPD features from surface species adsorbed on zig-zag structures would be more intense, and appear at higher temperatures than those from arm-chair structures.

Despite the complexity of the surface structure and the large number of variables involved in the desorption energy, it can be assumed that surface species of the same type, adsorbed on different sites, desorb in the same temperature range. Some qualitative trends, thus, can be established. For example it is expected to be easier to break external carbon-carbon bonds (~ 80 kcal/mol), than internal graphitic ones (~ 115 kcal/mol); and that at temperatures below 1200°C , carbon-oxygen single bonds can be thermally dissociated (~ 85 kcal/mol), but double bonds cannot (~ 175 kcal/mol).

Based on the TPD features observed, three types of surface species can be suggested after adsorption of CO , CO_2 , H_2O and O_2 on graphite. The low temperature ($100\text{--}400^{\circ}\text{C}$) CO precursor observed after CO adsorption, the high temperature CO precursor ($700\text{--}1000^{\circ}\text{C}$) observed after adsorption of all four gases and the CO_2 precursor ($200\text{--}600^{\circ}\text{C}$) also observed after adsorption of all four gases.

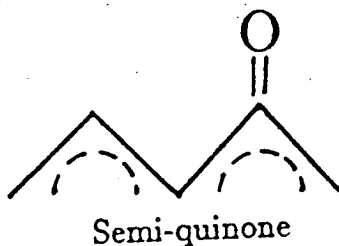
The low temperature CO precursor is likely due to weakly bound species such as carbonyl and/or ether groups. The low desorption

temperature of this species suggest that no graphitic carbon-carbon bonds are broken during the process.



To our knowledge, carbonyl species adsorbed on carbon have never been cited in the literature before, but analogy with CO adsorption on single crystal-metal surfaces [30] makes them favorable candidates. The transformation into ether groups is only a ring closure and appears energetically favored. The lack of spectroscopic data, however, prevents any further definition.

The high temperature CO precursor is assigned to a semi-quinone species.



The high stability of quinone groups in polycyclic aromatic compounds [36] gives strong support to the existence of semi-quinone

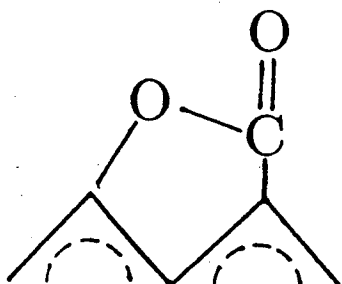
groups on the graphite surface. The desorption of this species involves the breaking of two carbon-carbon bonds in the graphite lattice, and explains the high desorption temperature. In the case of CO_2 , H_2O and O_2 adsorption, this species might be formed by reaction between an oxygen atom and a carbon atom, but in the case of CO adsorption there is no dissociation, and this species is formed by insertion of a molecule in the graphite lattice. This insertion requires a graphitic carbon-carbon bond breaking both for the formation and desorption of the species and justifies why the formation is such a highly activated process and why the desorption occurs at such high temperatures.

Although proposed earlier by several authors [12,13,15,16,17], hydroxyl or phenol groups do not appear to be good candidates for surface species after H_2O adsorption, based on our TPD results. The high similarities on the CO desorption signal, after exposures to either O_2 , CO_2 , CO or H_2O is a good indication that the same type of species (possibly a semi-quinone) is produced in all cases, as Kelemen and Freund pointed out [10]. The keto-enolic equilibrium, totally displaced towards the ketonic form for polycyclic aromatic compounds of high order [36] is another argument in favor of the nonexistence of phenol groups on the graphite surface.

At this point it is important to make a comment about the nomenclature used to identify these species. The name carbonyl has been employed to identify the low temperature CO species, rather than ketone, in agreement with IUPAC rules [37]. It must not be confused with the CO high temperature species. Most authors refer to this high temperature

species as carbonyl, but a more specific determination, such as ketone or oxo [38], or better semi-quinone, has been chosen in this work, in order to emphasize the strong conjugation with delocalized electrons as encountered in quinoid structures.

The CO_2 precursor is assigned to a lactone group.



Lactone

The formation of CO_2 from the decomposition of this species is analogous to decarboxylation reactions, which are very well known in organic chemistry [39]. This chemical species has been proposed by several authors [6,8,13,25], and the TPD results presented here suggest the existence of five different adsorption sites for this species, having activation energies for desorption ranging from 26 to 53kcal/mol.

Based on the results presented, a general scheme for the desorption products after O_2 , CO_2 , H_2O and CO is proposed (figure T). In all the cases studied, the desorption of CO at high temperatures is the main feature in the TPD experiments. It is then proposed that the main pathway for adsorption of the reactants is the formation of the high

temperature precursor species, possibly the semi-quinone. The activation energy for adsorption depends on the molecule itself, the site on which it adsorbs, and the coverage. O_2 dissociates to give two CO precursors, CO_2 yields a CO precursor and a gaseous CO molecule, and H_2O produces two hydrogen atoms which can either recombine (more probable event) or form carbon-hydrogen bonds (less probable event). The latter bonds can be benzenic like, and desorb as H_2 around $1000^{\circ}C$, or aliphatic-like and yield hydrocarbons at lower temperatures.

If the temperature is lower, say below $600^{\circ}C$, thermal decomposition of the CO precursor cannot occur, and only the formation of the CO_2 precursor (lactone group) is possible. The total oxygen scrambling observed after O_2 and CO_2 adsorption can be explained by an equilibrium between the CO and CO_2 precursors in the presence of the reactant gas. Since in the TPD experiments the amount of CO desorbed is much higher than the amount of CO_2 , this equilibrium is probably shifted to the formation of the more stable CO precursor.

More spectroscopic data is now necessary in order to support the assignment of the two CO and the CO_2 precursors to a carbonyl, a semi-quinone and a lactone group respectively. Vibrational techniques such as infrared, Raman or high resolution electron energy loss spectroscopy (HREELS) under UHV conditions can bring fruitful indications.

In all cases studied, the sticking coefficient of the gases is very low. The highest coverages, at a given exposure, were obtained after O_2 chemisorption, and even in this case no changes in the C_{1s} XPS peaks were observed when compared with the clean graphite. This indicates that only a few percent of the total carbon atoms have

chemisorbed oxygen even after high exposures (250Torr for 60s at 500⁰C), suggesting that the adsorption is highly activated.

Despite the low coverages, strong TPD signals were observed. From these signals, in principle, activation energies of adsorption can be determined, by studying variations of coverage with adsorption temperature, at a given exposure. In practice the inprecision in the intensity measurements of a group of broad and overlapping peaks makes accurate determinations difficult. Some qualitative information, however, can still be obtained. For example, for O₂ chemisorption the 820⁰C CO peak varies in intensity with temperature and the 980⁰C peak is almost insensitive (figure P) while in the case of CO₂ chemisorption, the change in intensity of the 980⁰C peak with adsorption temperature is larger than with the 820⁰C peak. This indicates that the activation energy for adsorption are dependent on both the type of molecule and type of site.

The physical wetting of clean graphite by liquid H₂O favors the formation of different surface species than the adsorption of H₂O vapor. After physical wetting, the amount of H₂O adsorbed is much higher. This is clearly shown by the appearance of a shoulder at 287eV in the C_{1s} XPS signal, which amounts to 20% of the carbon signal (figure R). In contrast, the signal obtained after H₂O vapor adsorption is the same as that of clean graphite, indicating that in this case a very small fraction of the carbon atoms interact with H₂O. The position of the shoulder after physical wetting is characteristic of slightly oxidized carbon atoms in compounds such as alcohol or ethers. The O_{1s} signal (figure Q) shows a large peak centered at 533eV. This

value is 1eV higher than that observed after O_2 and CO adsorption, and indicates a weaker electron transfer from the carbon to the oxygen atom, which is consistent with the C_{1s} result.

The desorption at rather low temperatures ($350^{\circ}C$)(figure S), giving H_2O as the main component, suggests again a weakly bound type of species. Phenolic groups can be ruled out since they would show an O_{1s} signal at lower binding energies (531eV), and the recombination of a C-OH and C-H groups to recover the H_2O molecule should occur at much higher temperatures, since it involves the breaking of a benzenic like carbon-hydrogen bond. The proposed species is a solvate between H_2O and the edge carbon atoms with bond energies about 35kcal/mol, as given by the desorption temperature [33].

After heating above $400^{\circ}C$, the O_{1s} binding energy shifts toward 532eV. This indicates that a fraction of the chemisorbed H_2O is able to dissociate and form CO precursor type species on the surface. The intensity of this signal is higher than that observed after H_2O vapor adsorption, and shows that physical wetting increases the H_2O dissociative chemisorption.

The reaction of H_2O with graphite is of great interest for the gasification of carbon solids. High temperature non-catalyzed reactions to give CO and H_2 probably proceeds following the high temperature route of figure T, that is via the formation of the CO precursor and by H_2 recombination.

To lower the temperature required to run this process, ways to facilitate the formation of the CO_2 precursor and its further decomposition must be found. Also of great importance and probably

related to the previous point, is the accessibility of the H_2O molecule to the active sites on the graphite-grain edges. XPS studies show that the H_2O vapor, at least at room temperature, cannot wet the surface in a significant fashion, whereas physical H_2O wetting covers 20% of the total number of sites (figures Q and R). One must therefore find ways to increase the surface wettability (sticking coefficient) by decreasing the activation energy for adsorption. There is no doubt that KOH, apart from other possible catalytic properties, can provide such an action owing to its hydrophilic properties. Additional TPD and XPS measurements must be undertaken systematically on the graphite/KOH system in order to obtain a better understanding of the catalytic reaction mechanism. Preliminary experiments on this system tend to demonstrate that the catalyst does not change the decomposition temperature but rather enhances dramatically the intensities of the TPD peaks, that is, the chemistry does not change and only the H_2O sticking coefficient increases. If confirmed, these observations would be of great interest.

REFERENCES

- [1] G. Blyholder and H. Eyring, J. Chem Phys 62, 1004 (1959) .
- [2] N.R. Laine, F.J. Vastola and P.L. Walker, J. Phys. Chem. 67, 2030 (1963).
- [3] P.J. Hart, F.J. Vastola and P.L. Walker, Carbon 5, 363 (1967).
- [4] R.C. Bansac, F.J. Vastola and P.L. Walker, J. Colloids and Interf. Sci., 32, 187 (1969).
- [5] A. Cheng and P. Harriot, Carbon 24, 143 (1986).
- [6] P.D. Koenig, R.G. Squires and N.M. Laurendeau, Carbon 23, 531 (1985).
- [7] A.M. Youssef, T.M. Ghazy and T.H. El-Nabarawy, Carbon 20, 113 (1982).
- [8] T.J. Fabish and D.E. Schleifer, Carbon 22, 19 (1984).
- [9] S.R. Kelemen and H. Freund, Carbon 23, 619 (1985).
- [10] S.R. Kelemen and H. Freund, Carbon 23, 723 (1985).
- [11] H. Hazdi and A. Novak, Trans. Farad. Soc., 51, 1614 (1955).
- [12] R.N. Smith, D.A. Young and R.A. Smith, Trans. Farad. Soc., 62, 2280 (1966).
- [13] C. Ishizaki and I. Marti, Carbon, 19, 409 (1981).
- [14] M.S. Akhter, J.R. Keifer, A.R. Chughtai and D.M. Smith, Carbon, 23, 589 (1985).
- [15] T. Takahagi and I. Ishitani, Carbon, 22, 43 (1984).
- [16] D.T. Clark and R. Wilson, Fuel, 62, 1034, (1983).
- [17] D.L. Perry and A. Grint, Fuel, 62, 1024 (1983).
- [18] S.R. Kelemen, H. Freund and C.A. Mims, J. Vac. Sci. Technol. A, 2, 987 (1984).
- [19] H. Harker, J.B. Horsley and D. Robson, Carbon, 9, 1 (1971).
- [20] H. Marsh and T.E. O'Hair, Carbon, 7, 703 (1969).
- [21] L. Bonnetain, J. Chim. Phys, 58, 34 (1961).
- [22] F.J. Vastola, P.J. Hart and P.L. Walker, Carbon, 2, 65 (1964).

- [23] F.S. Feates and C.W. Keep, *Trans. Farad. Soc.*, 66, 3156 (1970).
- [24] J. Dollimore, C.M. Freedman, B.H. Harrison and D.F. Quinn, *Carbon*, 8, 587 (1970).
- [25] S.S. Barton, G.L. Boulton and B.H. Harrison, *Carbon*, 10, 395 (1972).
- [26] A. Sen and J.E. Bercaw, *J. Phys. Chem.*, 84, 465 (1980).
- [27] Y. Matsumura, K. Yamabe and H. Takahashi, *Carbon*, 23, 263 (1985).
- [28] J.A. Britten, J.L. Falconer and L.F. Brown, *Carbon*, 23, 627 (1987).
- [29] S. Ergun, *J. Phys. Chem.*, 60, 480 (1956).
- [30] G.A. Somorjai, CHEMISTRY IN TWO DIMENSIONS, Cornell University Press, Ithaca, New York 14850 (1981).
- [31] B.G. Tucker and M.F.R. Mulcahay, *Trans. Farad. Soc.*, 65, 274, (1969).
- [32] K. Wandelt, *Surface Sci. Reports*, 2, 1 (1982).
- [33] P.A. Redhead, *Vacuum*, 12, 203 (1962).
- [34] R.T. Sanderson, CHEMICAL BOND IN ORGANIC COMPOUNDS, Sun and Sand Publishers, Scottsdale, Arizona, USA (1980)
- [35] S.E. Stein and R.L. Brown, *Carbon*, 23, 105 (1985).
- [36] E. Clar, POLYCYCLIC AROMATIC HYDROCARBONS, Academic Press (1964).
- [37] IUPAC, NOMENCLATURE OF ORGANIC CHEMISTRY, Rule C321.2, Pergamon Press (1979).
- [38] IUPAC, NOMENCLATURE OF ORGANIC CHEMISTRY, Rule C3.1, Pergamon Press (1979).
- [39] W. Adam, J. Baeza and J.C. Liu, *J. Am. Chem. Soc.*, 94, 2000 (1972).

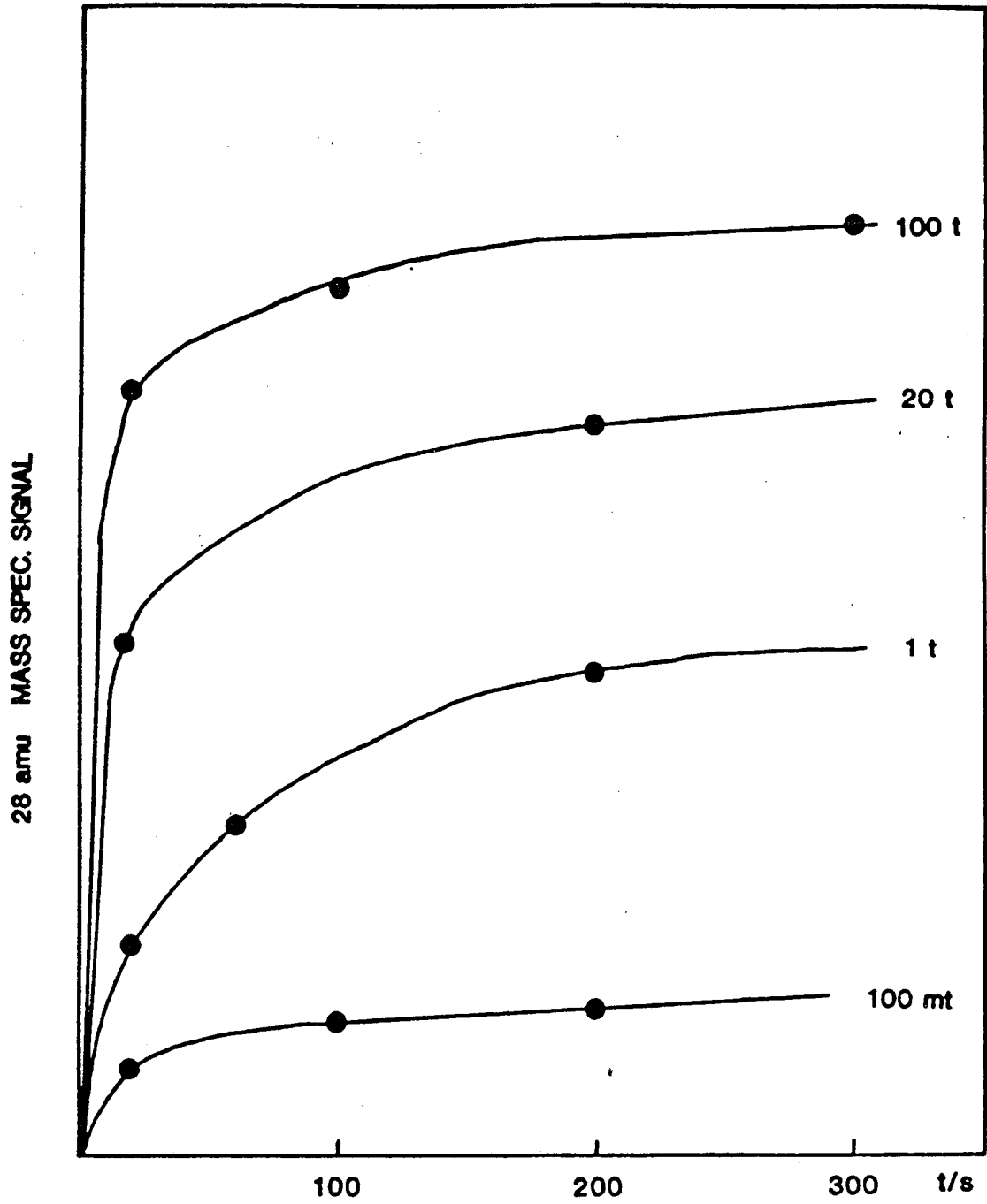


Figure A: CO adsorption kinetics on graphite at room temperature.

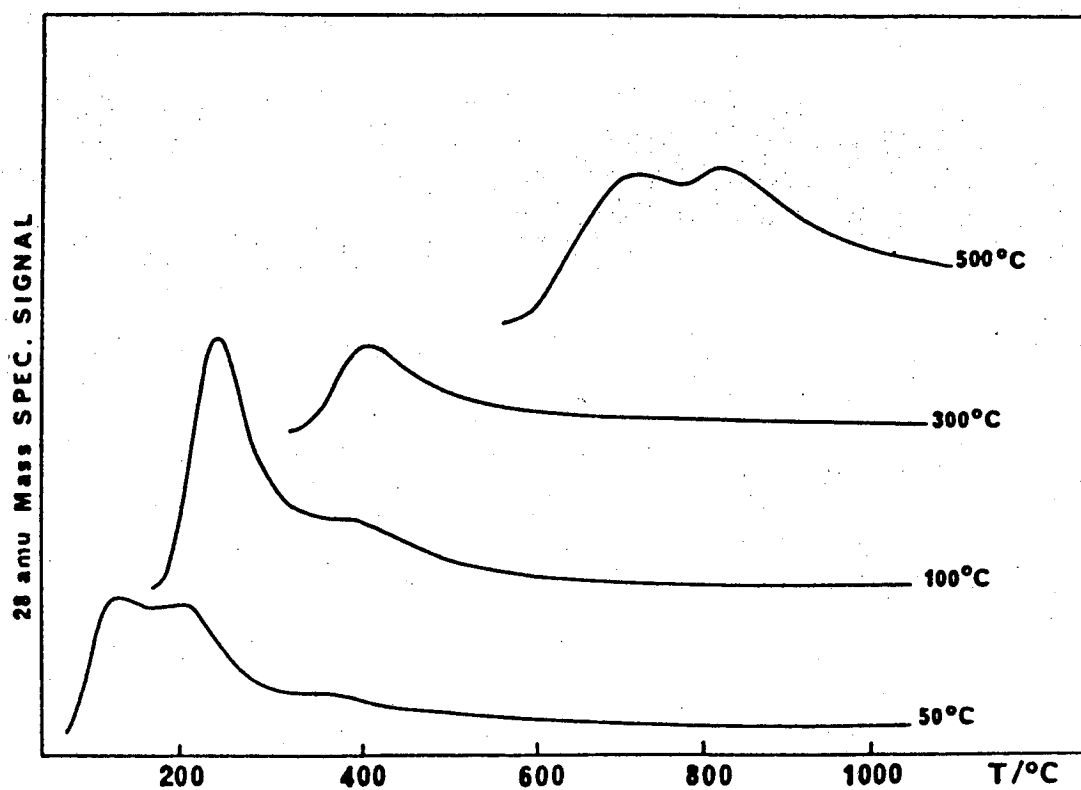


Figure B: Mass-28amu TPD spectra after 1800L (6×10^{-5} Torr for 30s) CO exposure to graphite at various temperatures.

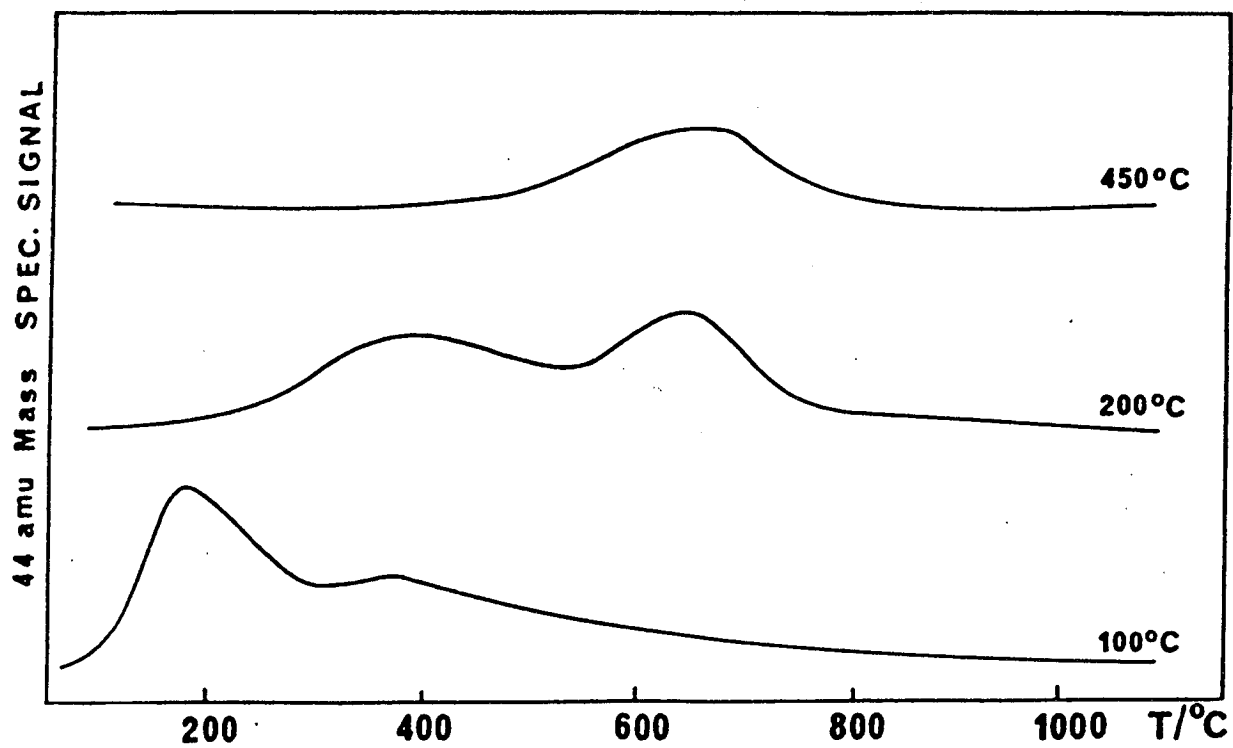


Figure C: Mass-44amu TPD spectra after 1800L (6×10^{-5} Torr for 30s) CO exposure to graphite at various temperatures.

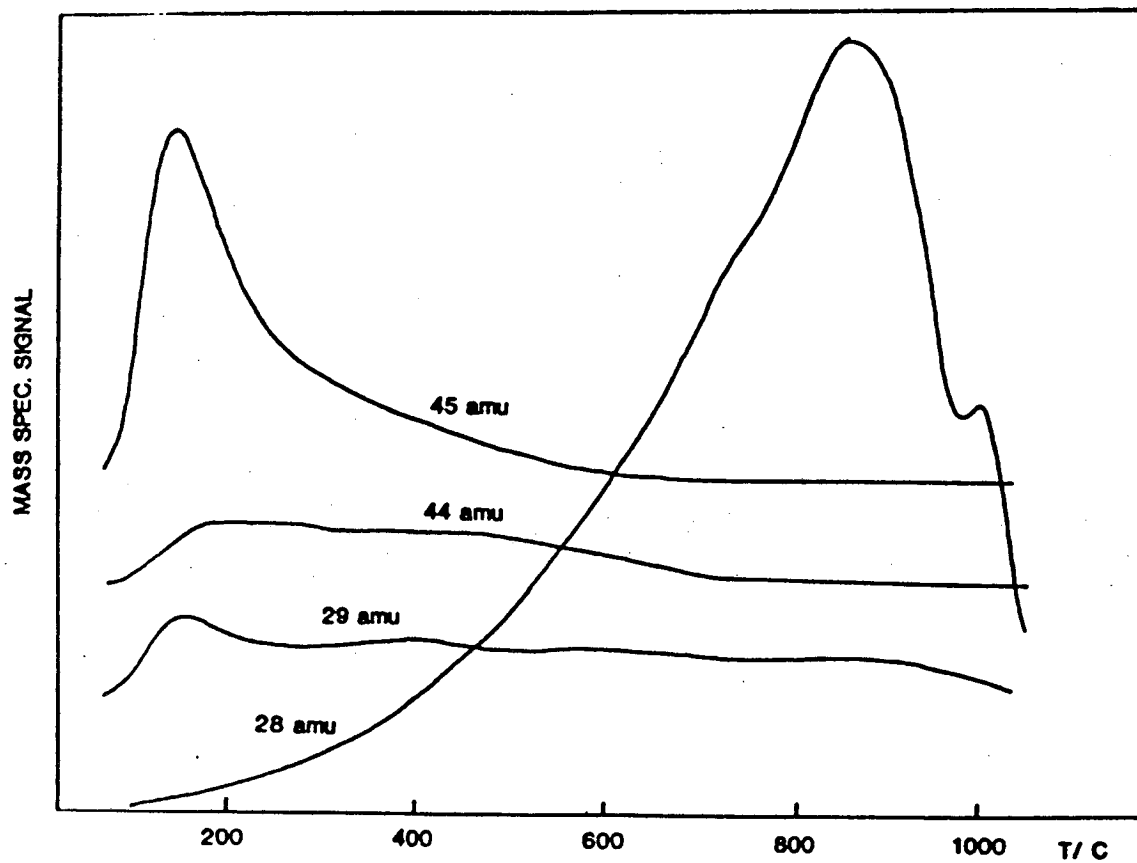


Figure D: TPD spectra after $^{13}\text{CO}_2$ exposure (8Torr for 60s) to graphite at room temperature.

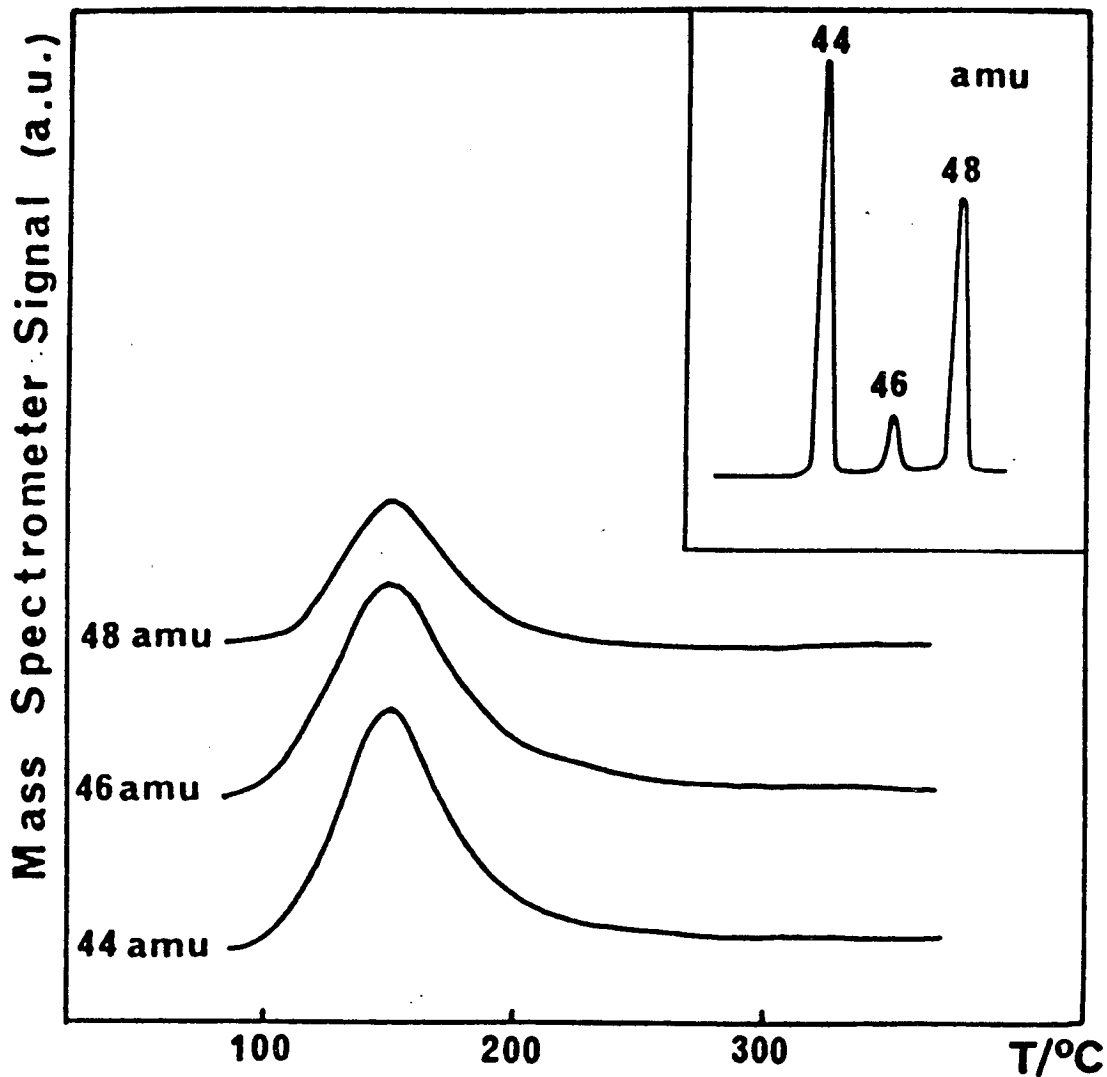


Figure E: (a) TPD spectra after 6000L exposure (2×10^{-4} Torr for 30s) of a $C^{16}O_2$ (58%)– $C^{18}O_2$ (42%) mixture to graphite at room temperature. (b) Mass spectrum of the mixture used for adsorption. The mass 46amu peak is ascribed to isotopic impurity.

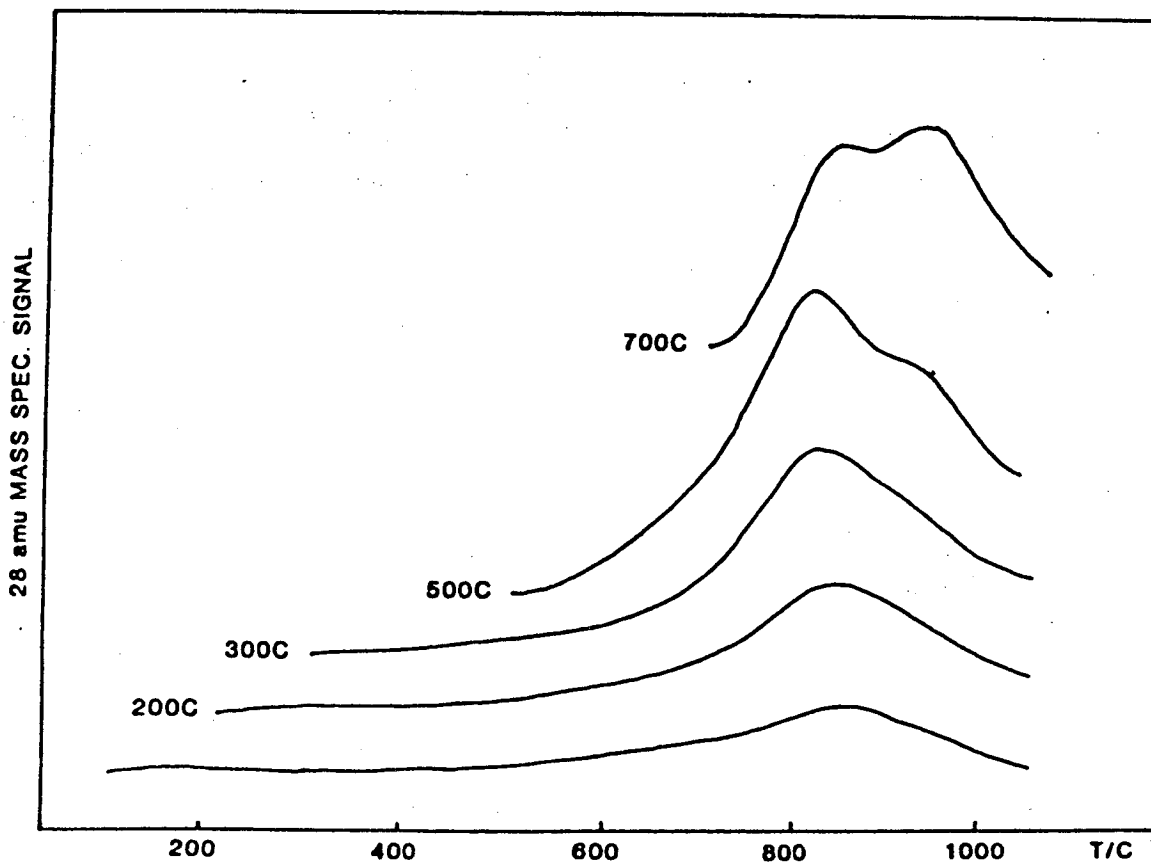


Figure F: Mass-28amu TPD spectra after 48000L (8×10^{-4} Torr for 60s) CO_2 exposure to graphite at various temperatures.

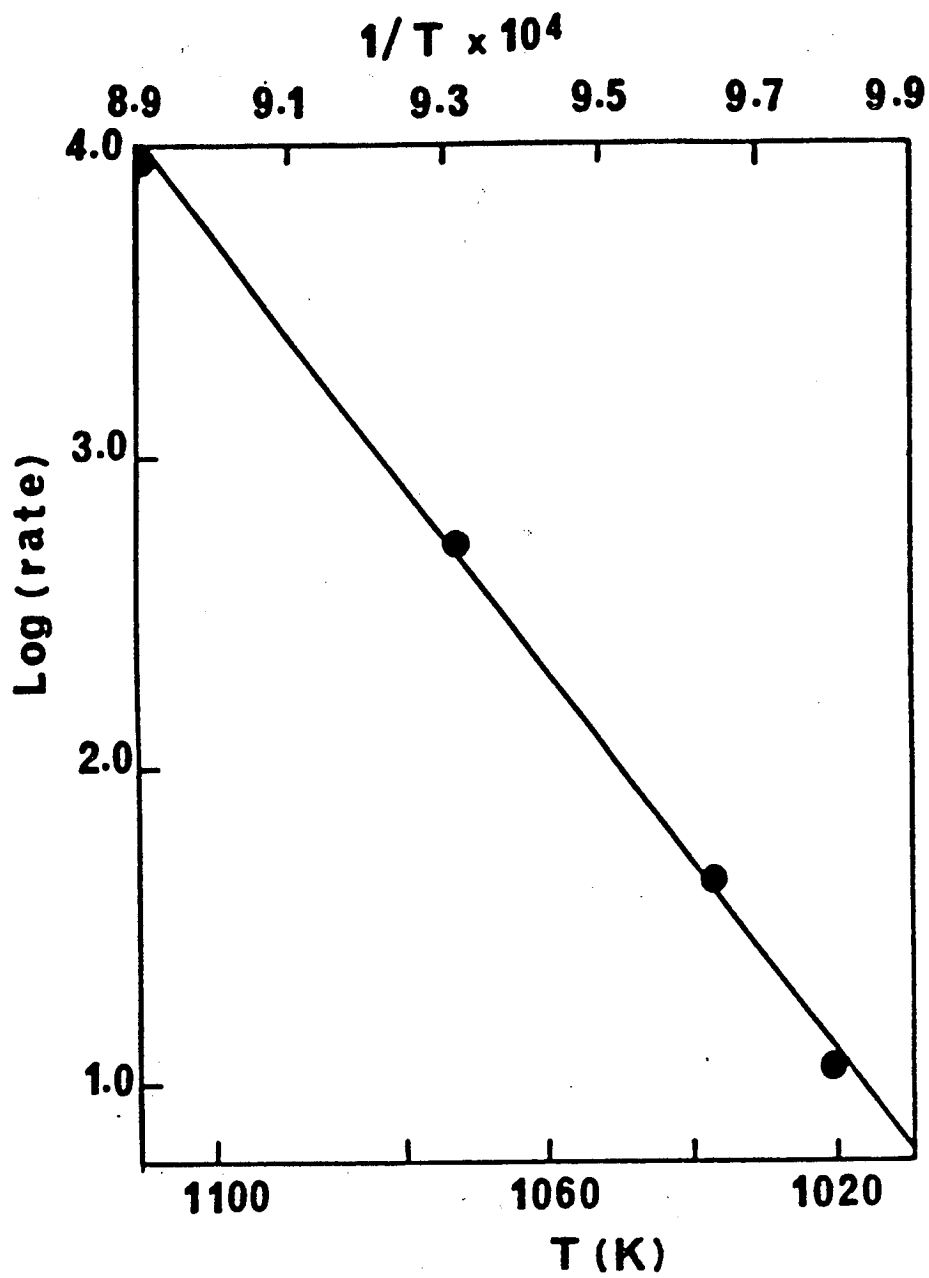


Figure G: Arrhenius plot for the $C + CO_2 \rightarrow 2 CO$ reaction.

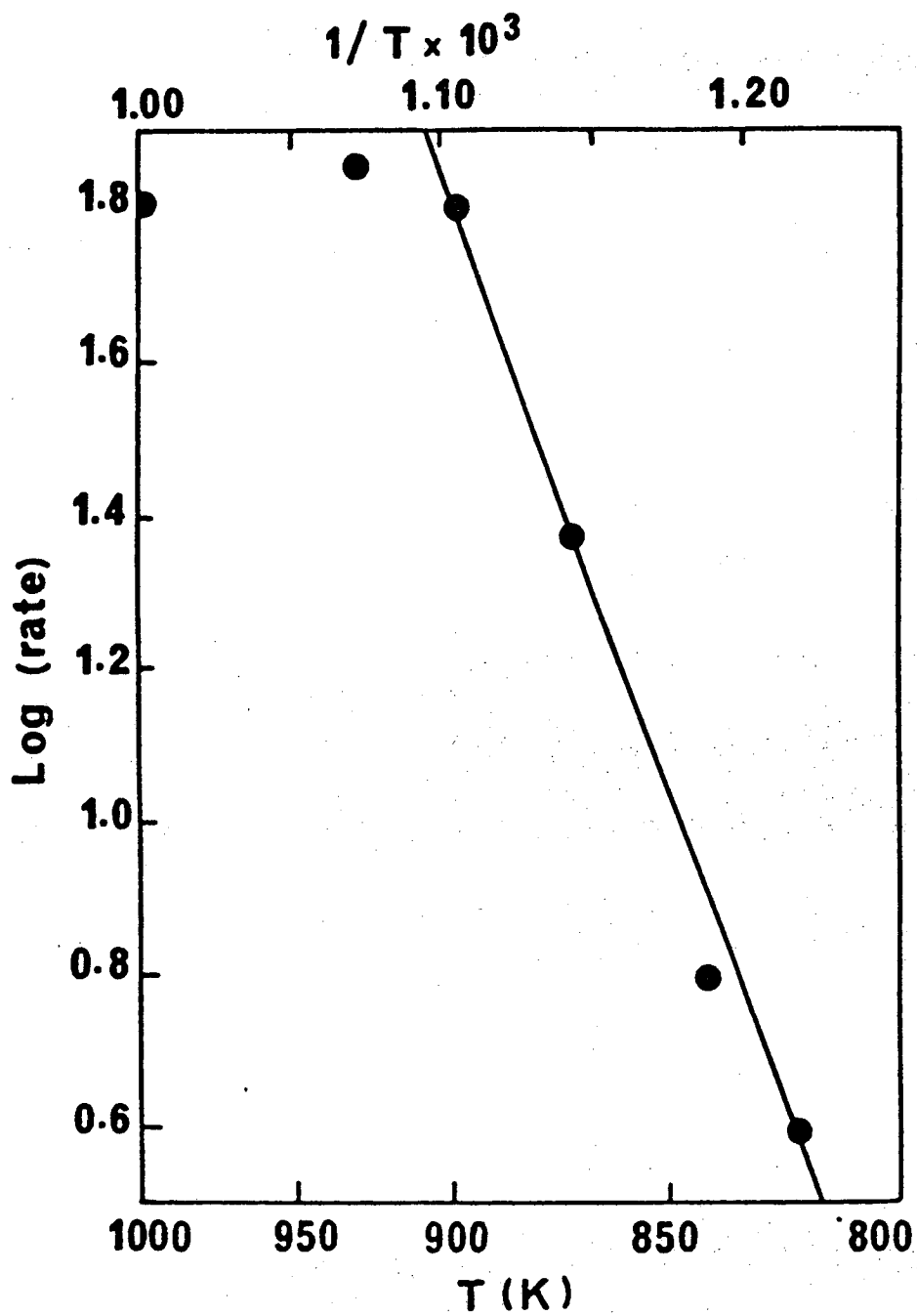


Figure H: Arrhenius plot for the $2 \text{ CO} \rightarrow \text{C} + \text{CO}_2$ reaction.

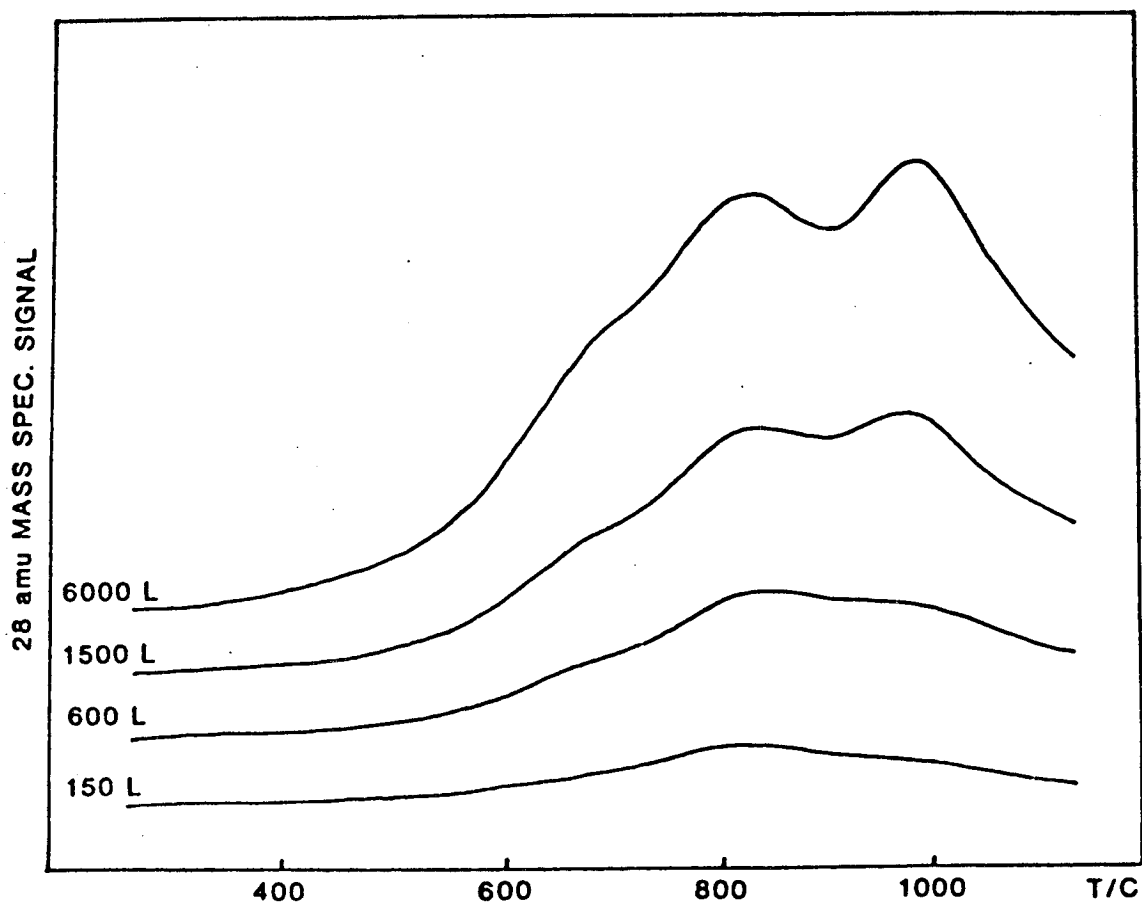


Figure I: Mass-28amu TPD spectra after adsorption of various O₂ doses on graphite at room temperature.

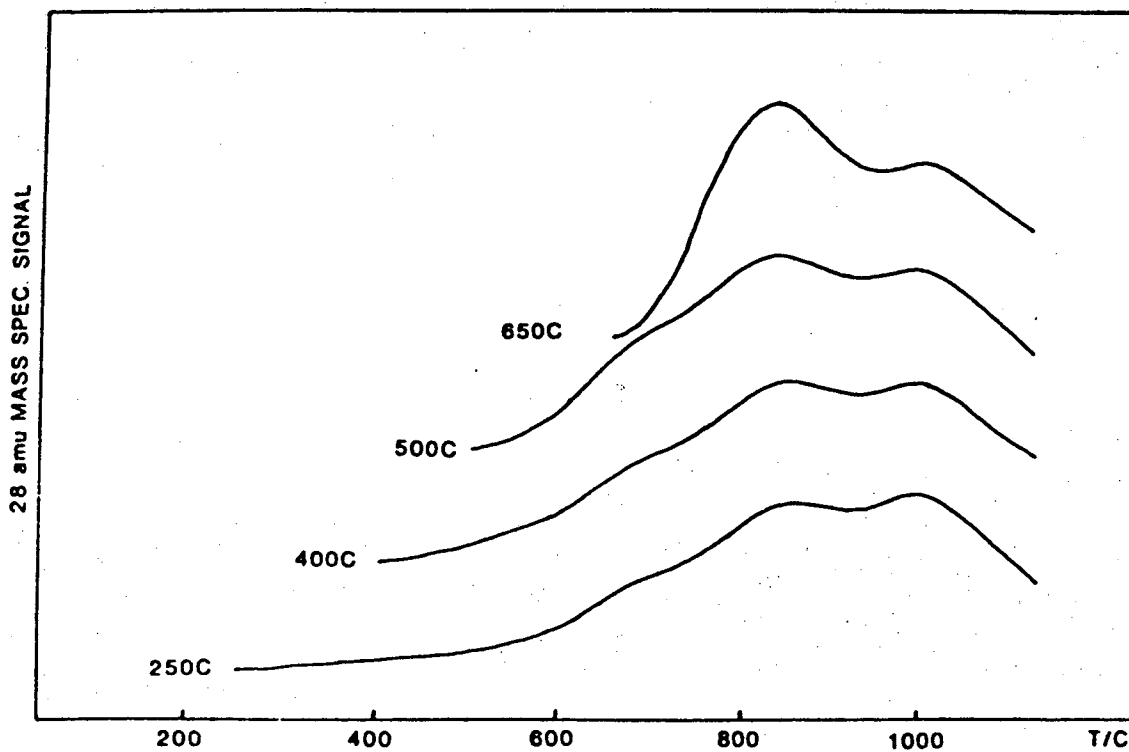


Figure J: Mass-28amu TPD spectra after 1500L (5×10^{-5} Torr for 30s) O_2 exposure to graphite at various temperatures.

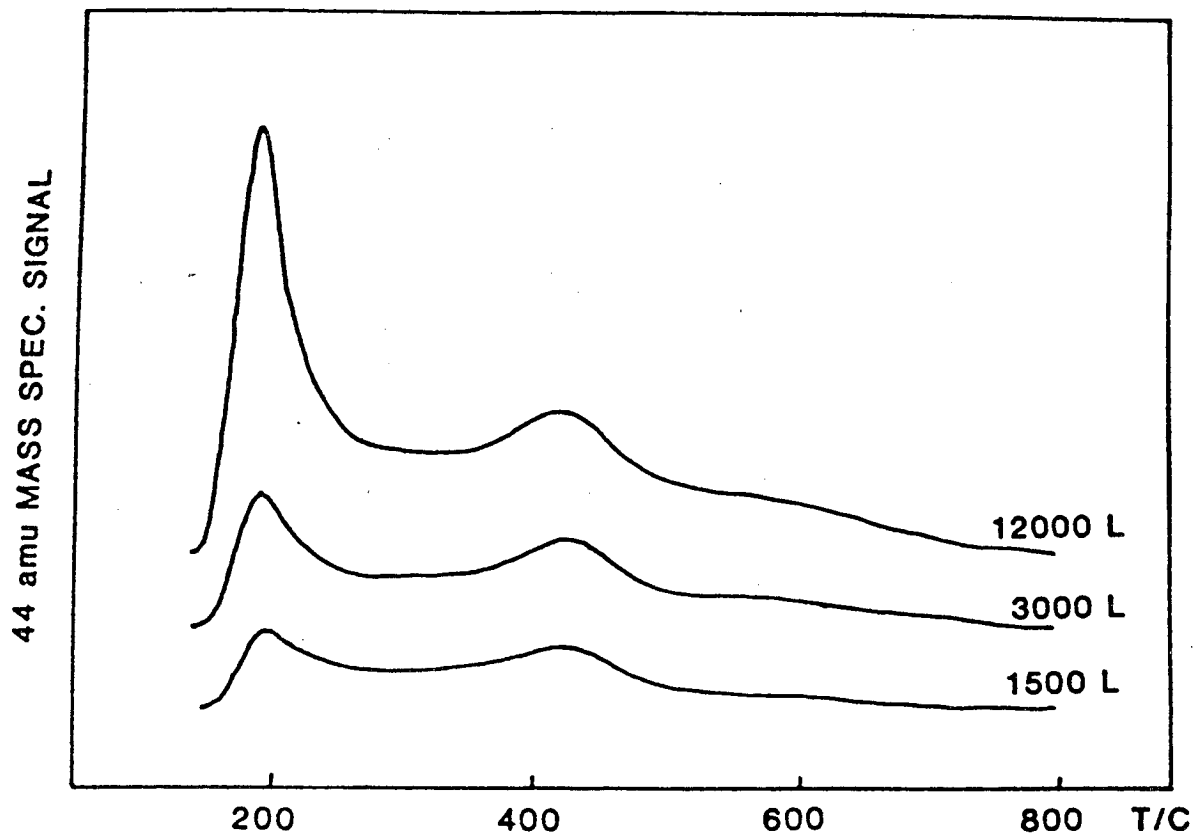


Figure K: Mass-44amu TPD spectra after adsorption of various O₂ doses on graphite at room temperature.

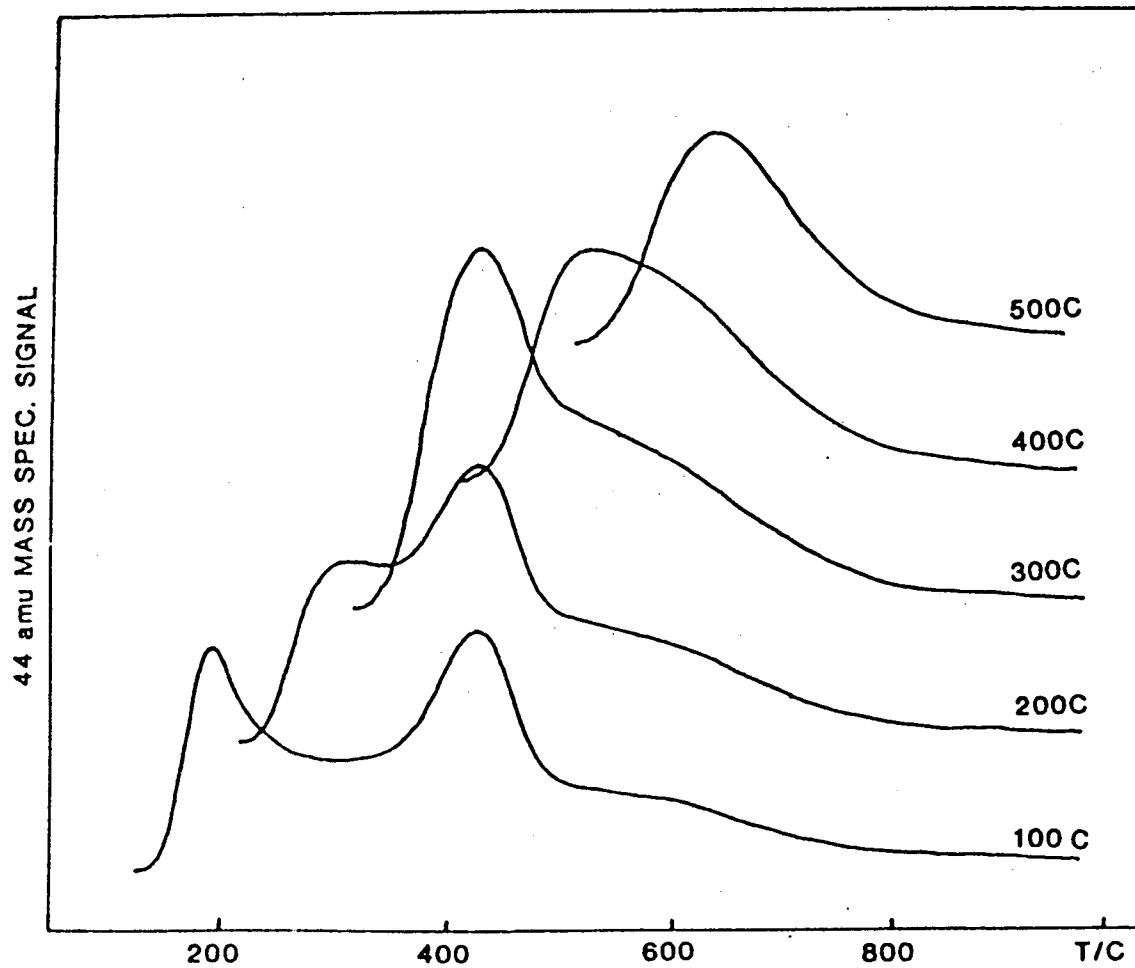


Figure L: Mass-44amu TPD spectra after 900L (6×10^{-5} Torr for 15s) O_2 exposure to graphite at various temperatures.

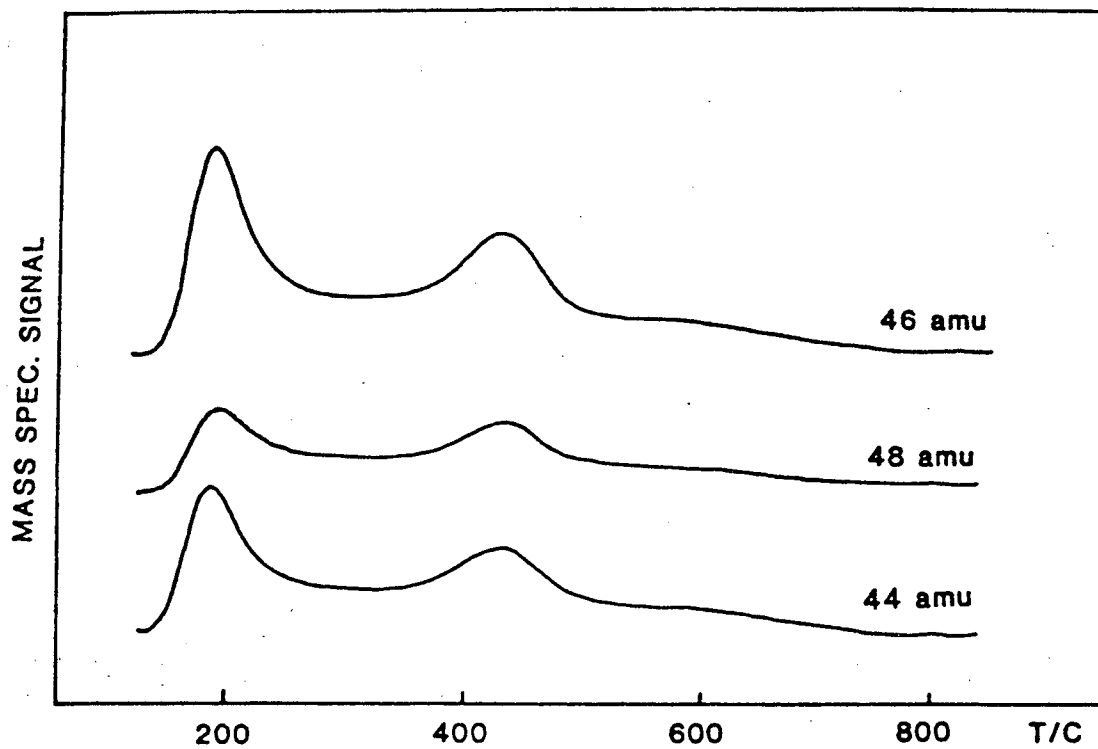


Figure M: TPD spectra after exposing a clean graphite surface to 900L (6×10^{-5} Torr for 15s) of a mixture of $^{16}\text{O}_2$ (53%) and $^{18}\text{O}_2$ (47%) at room temperature.

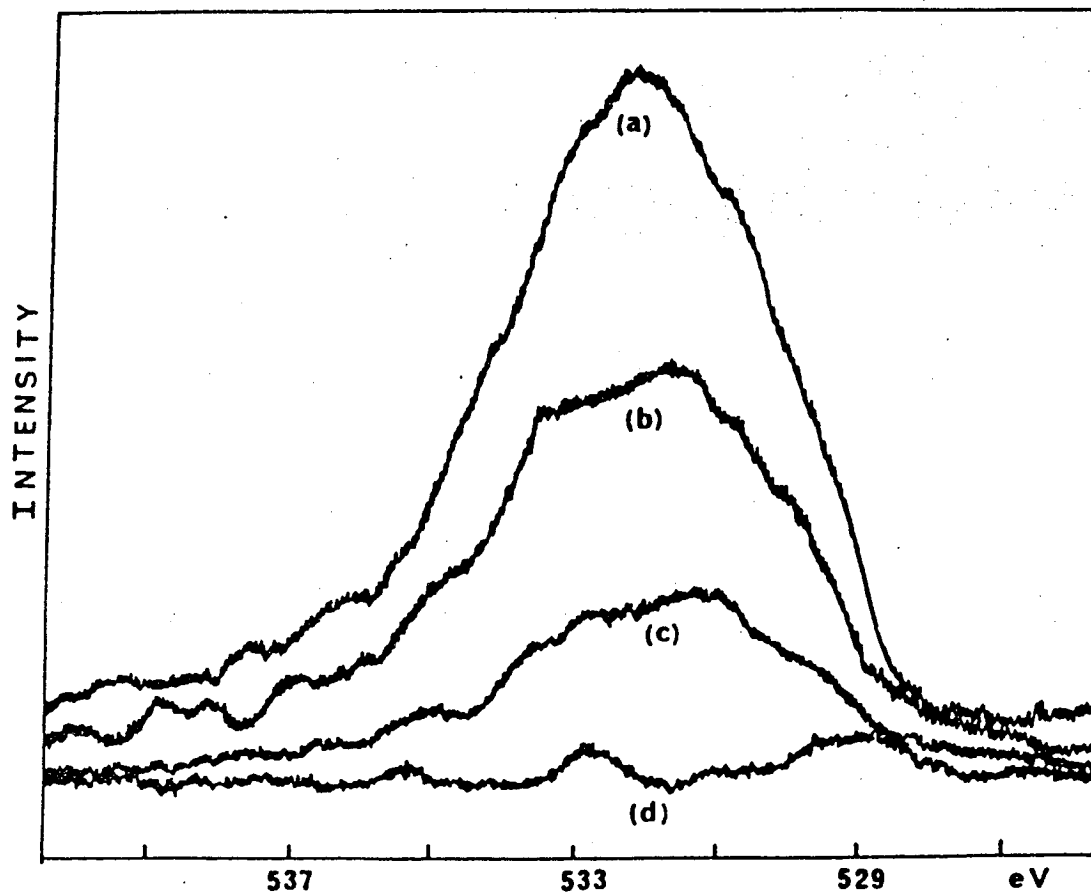


Figure N: O_{1s} XPS spectrum of the graphite surface, (a) after exposure to 250Torr of O₂ at 530°C for 5min, and after flash at (b) 720°C, (c) 840°C, and (d) 1080°C.

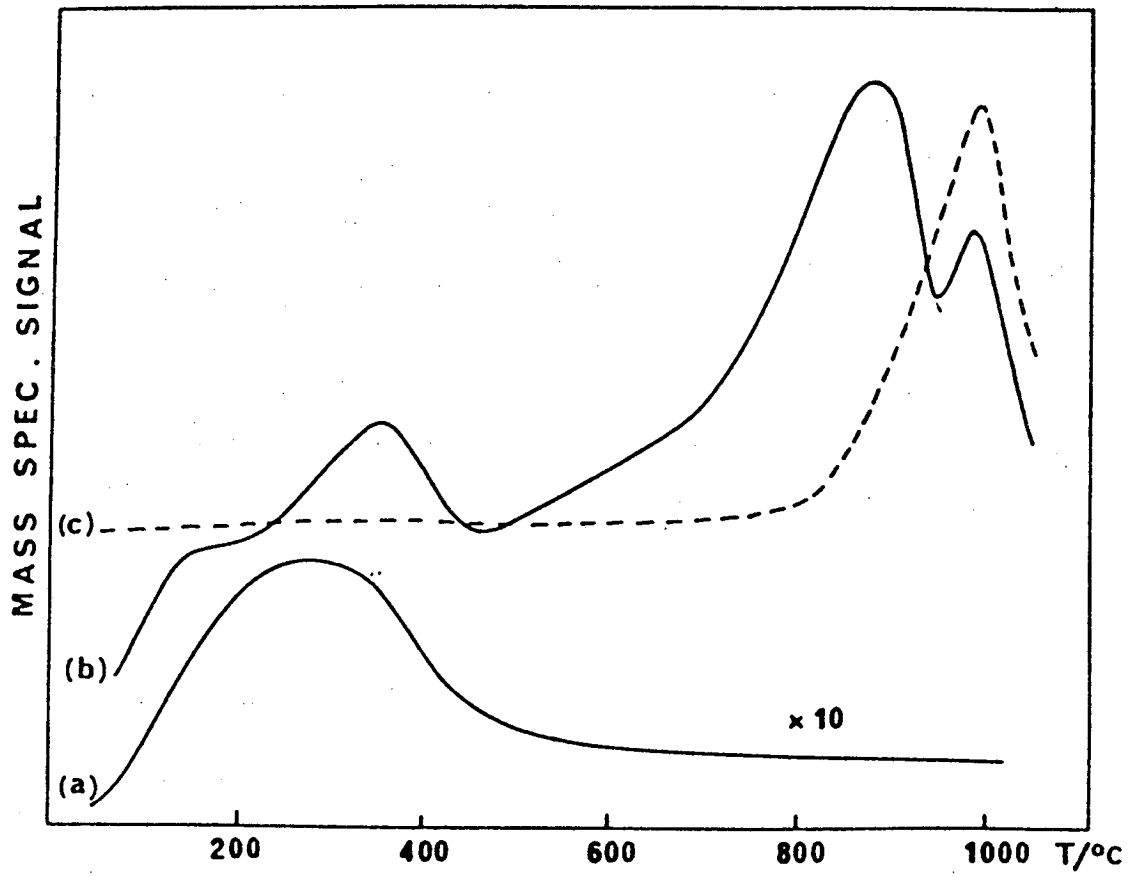


Figure 0: TPD spectra after exposing a clean graphite surface to 20Torr H₂O for 1min at room temperature. (a) mass 44amu, (b) mass 28amu and (c) mass 2amu.

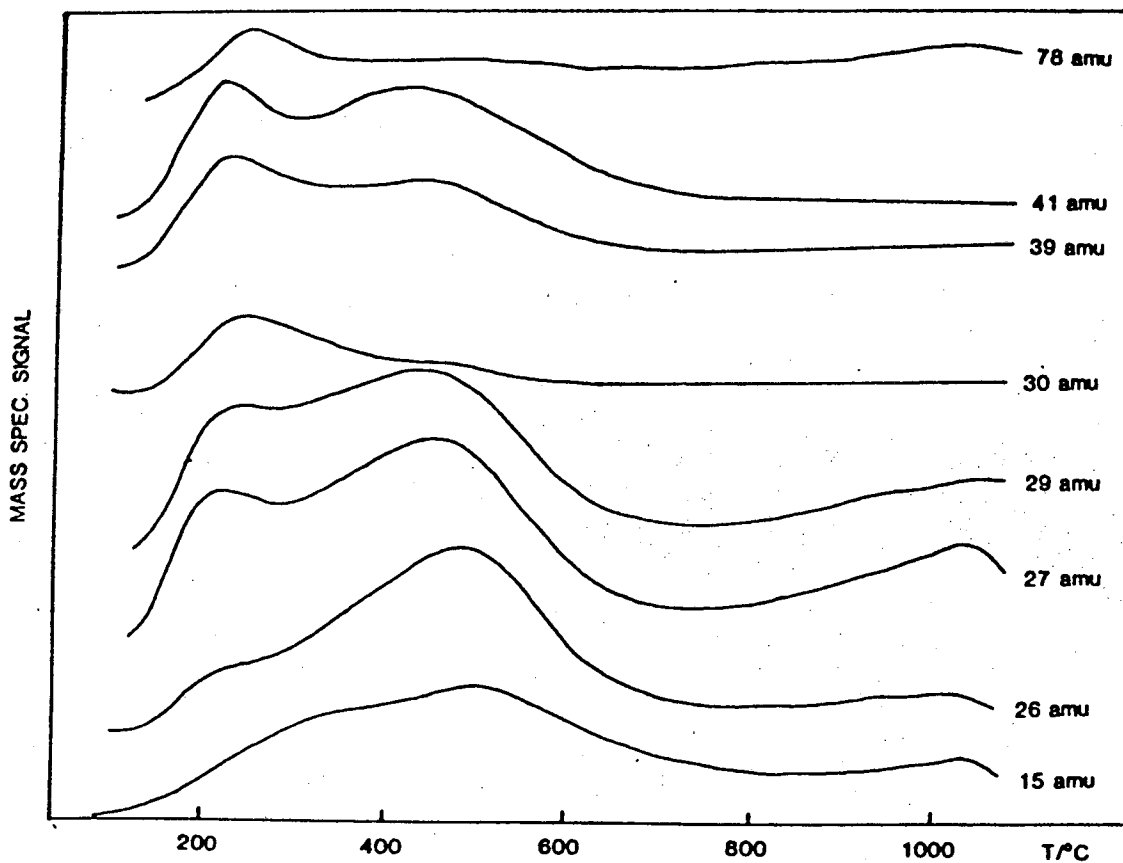


Figure P: TPD spectra after exposing a clean graphite surface to 20Torr of H_2O for 1min at room temperature. The scale is expanded by 10, compared with figure 6.15.

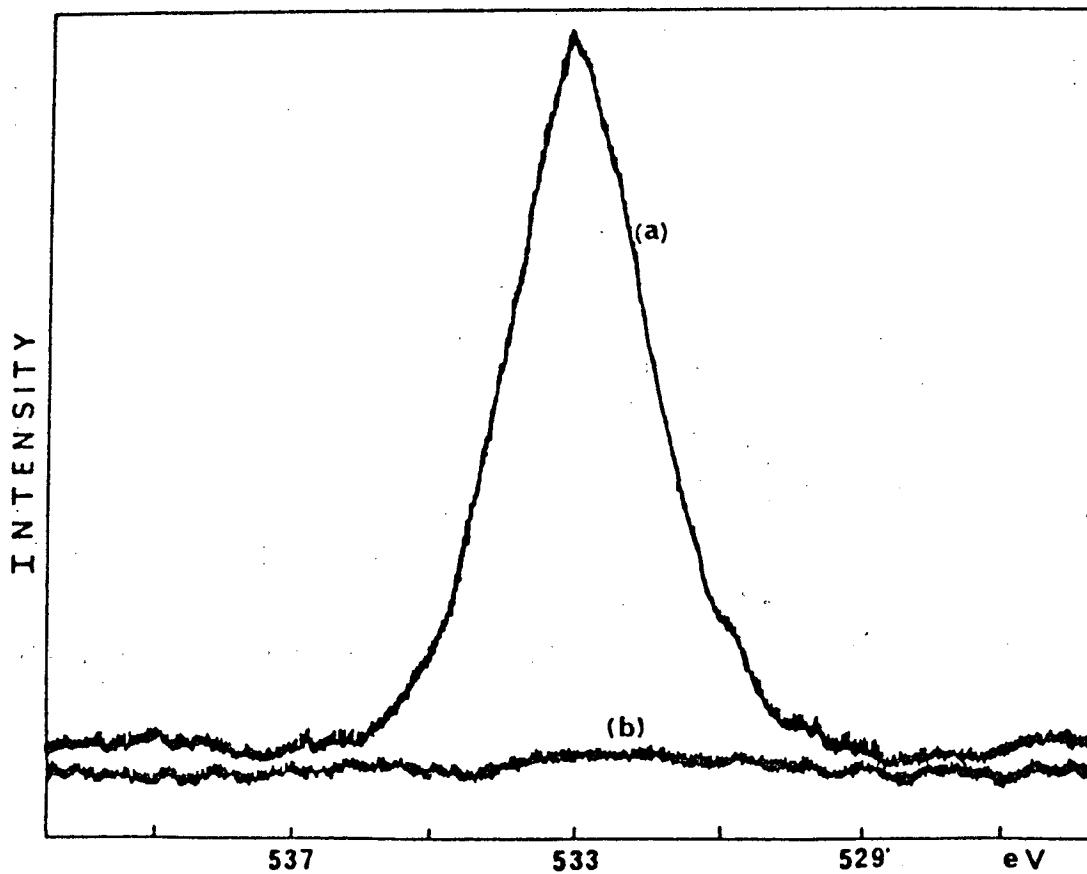


Figure Q: O_{1s}-XPS signal of a graphite surface after (a) wetting with H₂O and (b) exposure to 20Torr of H₂O vapor for 60s.

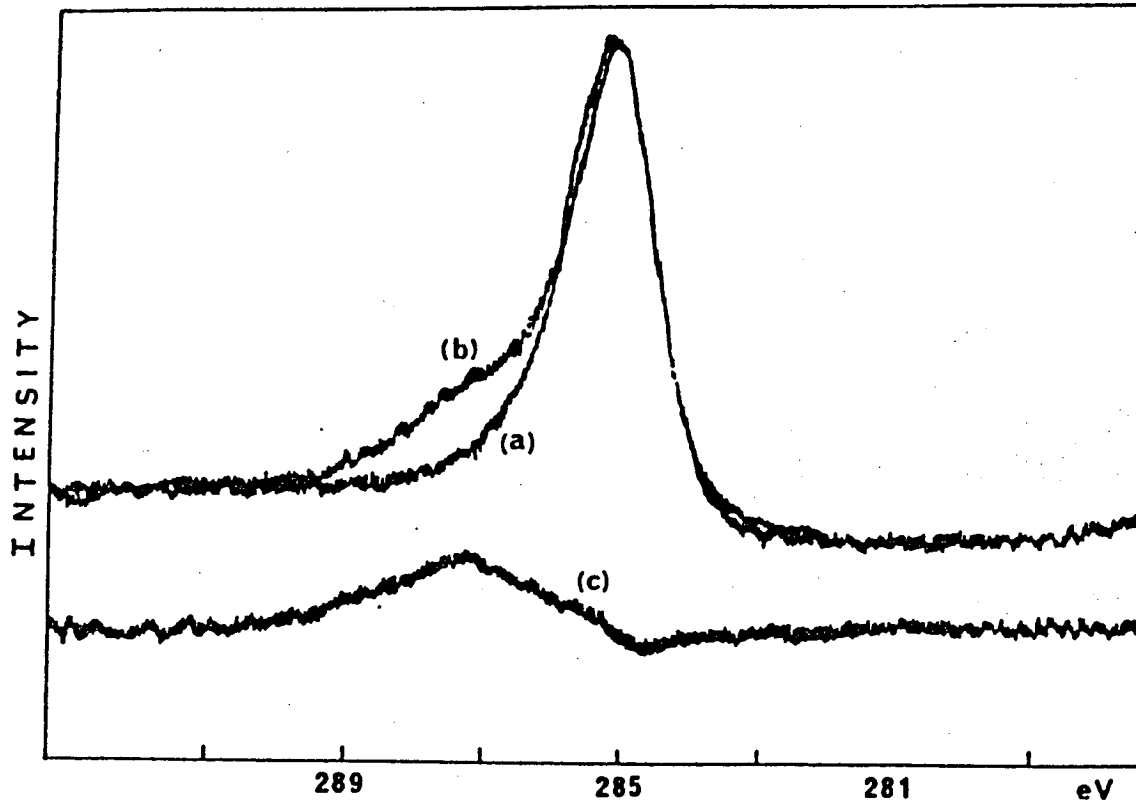


Figure R: C_{1s}-XPS signal of (a) a clean graphite surface, and (b) after wetting with H₂O. Curve (c) is the difference between curves (a) and (b).

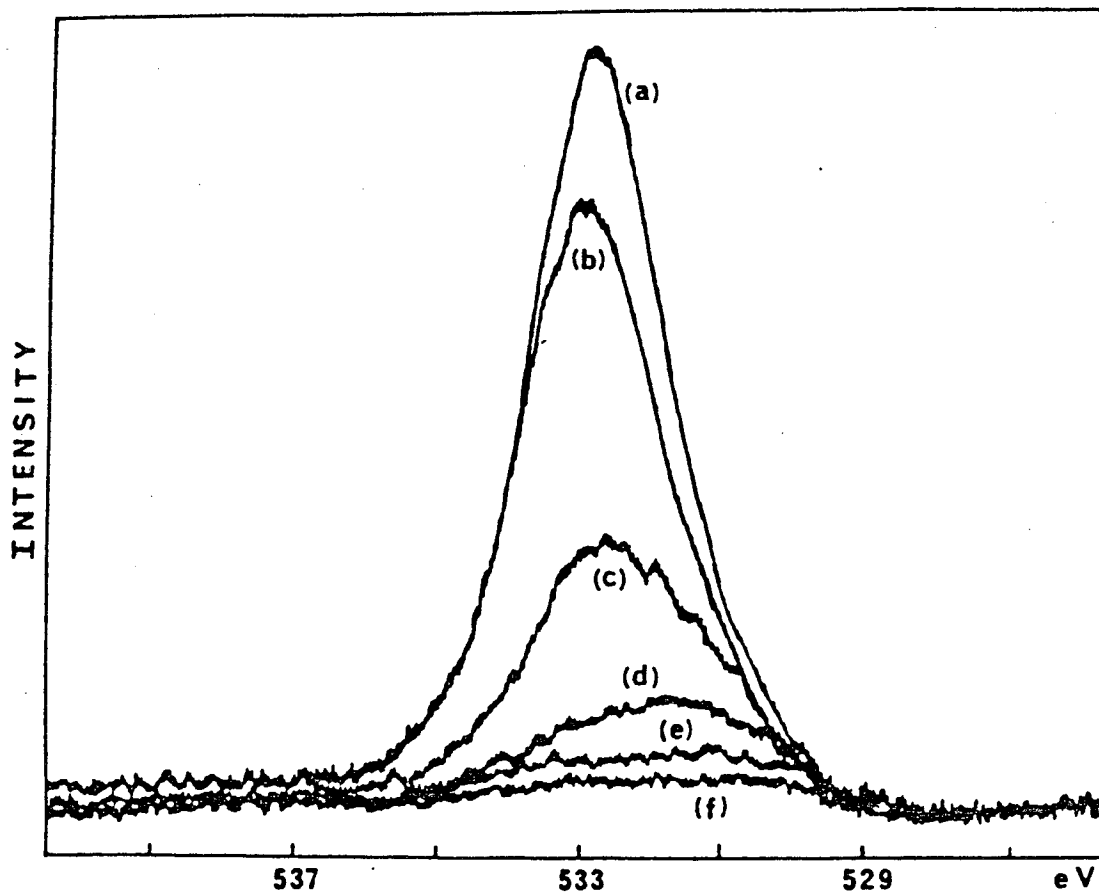


Figure S: O_{1s}-XPS signal of a graphite surface, (a) after surface wetting, and after flash at (b) 250°C, (c) 320°C, (d) 390°C, (e) 530°C and (f) 740°C.

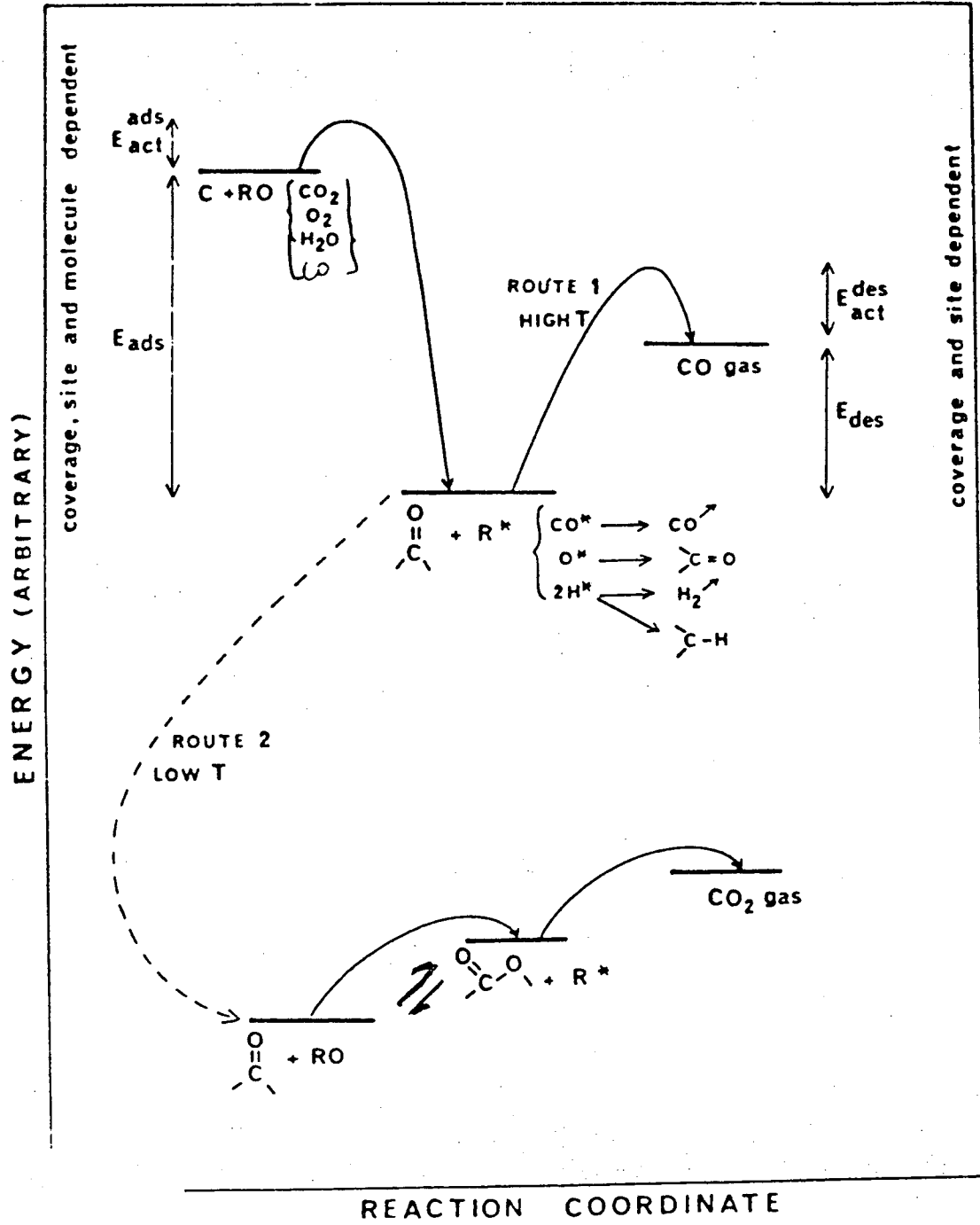


Figure T: General schematic mechanism for graphite gasification reactions.

Table 1: Desorption temperatures and activation energies for desorption of CO and CO₂ after adsorption of CO, CO₂, O₂ and H₂O.

Adsorption gas	Adsorption temp (°C)	Desorption product	Desorption temp (°C)	E_{des}^a (kcal/mol)
CO	> 500	CO	700-980	64-83
CO ₂	room temp			
O ₂	250-650			
H ₂ O	room temp			
CO	50-300	CO	120-400	25-44
CO	100-450	CO ₂	170-650	28-60
CO ₂	room temp		150	27
O ₂	250-650		190-650	28-60
H ₂ O	room temp		100-600*	21-51

* One broad feature.

LAWRENCE BERKELEY LABORATORY
TECHNICAL INFORMATION DEPARTMENT
UNIVERSITY OF CALIFORNIA
BERKELEY, CALIFORNIA 94720